▰ ◧ COORDINATED SCIENCE LABORATORY

APPROXIMATIONS TO
ROBUST WIENER FILTERS

DTIC
ELECTE
NOV 2 1 1985
D

UNIVERSITY OF ILLINOIS AT URBANA-CHAMPAIGN

11 18-85 028

AD-A161 331

REPORT DOCUMENTATION PAGE

1a. REPORT SECURITY CLASSIFICATION	1b. RESTRICTIVE MARKINGS
UNCLASSIFIED	
2a. SECURITY CLASSIFICATION AUTHORITY	3. DISTRIBUTION/AVAILABILITY OF REPORT
	UNLIMITED
2b. DECLASSIFICATION/DOWNGRADING SCHEDULE	

4. PERFORMING ORGANIZATION REPORT NUMBER(S)	5. MONITORING ORGANIZATION REPORT NUMBER(S)
R-1010	
UILU-ENG84-2204	

6a. NAME OF PERFORMING ORGANIZATION	6b. OFFICE SYMBOL (If applicable)	7a. NAME OF MONITORING ORGANIZATION
Coordinated Science Laboratory		Office of Naval Research

6c. ADDRESS (City, State and ZIP Code)	7b. ADDRESS (City, State and ZIP Code)
University of Illinois	800 N. Quincy
1101 W. Springfield Avenue	Arlington, VA 22217
Urbana, IL 61801	

DTIC
ELECTE
NOV 21 1985
S D

8a. NAME OF FUNDING/SPONSORING ORGANIZATION	8b. OFFICE SYMBOL (If applicable)	9. PROCUREMENT INSTRUMENT IDENTIFICATION NUMBER
Joint Services Electronics Program		N00014-79-C-0424

A

8c. ADDRESS (City, State and ZIP Code)	10. SOURCE OF FUNDING NOS.			
800 N. Quincy	PROGRAM ELEMENT NO.	PROJECT NO.	TASK NO.	WORK UNIT NO.
Arlington, VA 22217				

11. TITLE (Include Security Classification) APPROXIMATIONS TO ROBUST WIENER FILTERS

12. PERSONAL AUTHOR(S)
Myrna Roula Cotran

13a. TYPE OF REPORT	13b. TIME COVERED	14. DATE OF REPORT (Yr., Mo., Day)	15. PAGE COUNT
Technical	FROM _____ TO _____	May 4, 1984	68

16. SUPPLEMENTARY NOTATION

17.	COSATI CODES		18. SUBJECT TERMS (Continue on reverse if necessary and identify by block number)
FIELD	GROUP	SUB. GR.	Robust signal estimation; minimax design; finite-order filters

19. ABSTRACT (Continue on reverse if necessary and identify by block number)

Several approximations to the robust Wiener filters for two uncertainty classes of signal and noise spectra are considered. The approximations consist of realizable n-th order filters of the Butterworth and Chebyshev types. For each uncertainty class, the worst-case performances of the approximate and ideal robust filters are compared. It is found that, for the ε-contaminated uncertainty class, the approximate robust filter using only second-order Butterworth filters gives a very good approximation. For the p-point class, where there is more uncertainty in the knowledge of the true spectra of the signal and noise, it is necessary to use filters of relatively high orders to obtain good approximations. Furthermore for this class, the best approximation is obtained by using Chebyshev filters of high orders and small ripple.

20. DISTRIBUTION/AVAILABILITY OF ABSTRACT	21. ABSTRACT SECURITY CLASSIFICATION
UNCLASSIFIED/UNLIMITED ☒ SAME AS RPT. ☐ DTIC USERS ☐	UNCLASSIFIED

22a. NAME OF RESPONSIBLE INDIVIDUAL	22b. TELEPHONE NUMBER (Include Area Code)	22c. OFFICE SYMBOL

APPROXIMATIONS TO ROBUST WIENER FILTERS

BY

MYRNA ROULA COTRAN

B.S., University of Illinois, 1982

THESIS

Submitted in partial fulfillment of the requirements
for the degree of Master of Science in Electrical Engineering
in the Graduate College of the
University of Illinois at Urbana-Champaign, 1984

Urbana, Illinois

APPROXIMATIONS TO ROBUST WIENER FILTERS

Myrna Roula Cotran
Coordinated Science Laboratory and
Department of Electrical Engineering
University of Illinois at Urbana-Champaign, 1984

ABSTRACT

Several approximations to the robust Wiener filters for two uncertainty classes of signal and noise spectra are considered. The approximations consist of realizable n-th order filters of the Butterworth and Chebyshev types. For each uncertainty class, the worst-case performances of the approximate and ideal robust filters are compared. It is found that, for the ε-contaminated uncertainty class, the approximate robust filter using only second-order Butterworth filters gives a very good approximation. For the p-point class, where there is more uncertainty in the knowledge of the true spectra of the signal and noise, it is necessary to use filters of relatively high orders to obtain good approximations. Furthermore, for this class, the best approximation is obtained by using Chebyshev filters of high orders and small ripple.

ACKNOWLEDGMENT

TABLE OF CONTENTS

I. INTRODUCTION

The design of linear minimum mean-square-error (MMSE) estimation filters (or Wiener filters) for stationary signals in additive stationary noise requires precise knowledge of the signal and noise power spectral densities (PSD's). In practice, however, the actual signal and noise may differ to a certain degree from these nominal densities. This can lead to considerable degradation in the performance of Wiener filters.

A minimax solution to this problem was proposed by Poor [1], based on the work of Kassam and Lim [2]. To accommodate for the uncertainty, it is assumed that the spectral densities of the signal and noise lie in some general classes of possible spectra. A filter, termed "robust", is then designed to minimize the mean-square-error (MSE) for the "worst-case" pair of spectra in that class.

For many uncertainty spectral classes of interest, the robust filters are not physically realizable. Therefore, the purpose of this thesis is to find realizable (finite-order) filters which are good approximations of the ideal robust filters. Two uncertainty models for spectra will be considered: the ϵ-contaminated class and the p-point class. We will approximate the ideal robust filters with realizable n-th order filters composed of low-pass, high-pass, and all-pass Butterworth or Chebyshev analog filters. We will then analyze the performance of those filters and compare it to that of the ideal filters.

From the classical theory of Wiener filtering, the MSE associated with estimating a signal in uncorrelated additive noise, where the signal and noise are zero-mean, second-order, wide-sense stationary random processes is given by

$$e(S,N,H) = \frac{1}{2\pi} \int_{-\infty}^{\infty} [S(\omega)|1-H(\omega)|^2 + N(\omega)|H(\omega)|^2]d\omega \tag{1}$$

where $S(\omega)$ and $N(\omega)$ are the PSD's of the signal and noise, respectively, and $H(\omega)$ is the transfer function of the filter. For a given signal and noise spectral pair (S_0, N_0), the Wiener filter

$$H_0^*(\omega) = \frac{S_0(\omega)}{S_0(\omega)+N_0(\omega)} \tag{2}$$

minimizes the MSE. The corresponding minimum MSE is

$$e(S_0, N_0, H_0^*) = \frac{1}{2\pi} \int_{-\infty}^{\infty} H_0^*(\omega)N_0(\omega)d\omega \tag{3}$$

Throughout this study, we will be considering a nominal pair of spectral densities $S_0(\omega)$ and $N_0(\omega)$ to be the original pair used in designing the nominal Wiener filter. Specifically, we will assume we have a narrow-band, first-order Markov signal in wide-band, first-order Markov noise, i.e.,

$$S_0(\omega) = \frac{2a_S v_S^2}{a_S^2 + \omega^2} \tag{4.a}$$

and

$$N_0(\omega) = \frac{2a_N v_N^2}{a_N^2 + \omega^2} \tag{4.b}$$

where a_S and a_N are the 3 dB bandwidths and v_S^2 and v_N^2 are the total powers of the signal and noise processes, respectively. The corresponding nominal Wiener filter (using Equation (2)) is given by

$$H_0^*(\omega) = \frac{a_S r(a_N^2 + \omega^2)}{a_N a_S(a_S + a_N r) + (a_N + a_S r)\omega^2} \tag{5}$$

where $r \triangleq \dfrac{v_S^2}{v_N^2}$ is the input signal-to-noise ratio (SNR). Such a model is

reasonable to assume for many applications.

As we mentioned earlier, it has been shown that the performance of

the nominal filter H_0^* becomes unacceptable when the signal and noise PSD's

vary from the nominal densities given by (4.a) and (4.b) (see Vastola [3]).

A more realistic approach is to let the signal and noise be members of some

uncertainty classes of spectra $\mathscr{A}$ and $\mathcal{N}$. The robust filter H_R is a solution

to

$$\min_{H} \left[\sup_{(S,N) \in \mathscr{A} \times \mathcal{N}} e(S,N,H) \right] \tag{6}$$

i.e., it is the Wiener filter for the pair of spectra that has the maximum

MSE over that class. In this sense, the robust filter gives the smallest

upper bound on the MSE over the classes $\mathscr{A}$ and $\mathcal{N}$. Thus, it guarantees a

certain level of performance.

Since robust filters are derived without the constraints of physical

realizability, it is our objective to find realizable n-th order filters

such that, as the order n increases, their performances approach that of

the ideal robust filters. In Chapters II and III, we will consider robust

filters for two uncertainty classes of spectra: the ε-contaminated class

and the p-point class. For each class, we will approximate the ideal robust

filter transfer function with Butterworth or Chebyshev filters (which are

rational functions) and evaluate $\sup\limits_{(S,N)\in \mathcal{S}\times \mathcal{N}} e(S,N,H_n)$, where H_n is the n-th order approximate robust filter. We will compare the worst-case performance of H_n to that of the ideal robust filter H_R and the nominal filter H_0^*.

In our numerical results, performance will be measured in terms of output SNR versus input SNR. The output SNR will be taken to be the signal power divided by the MSE, i.e.,

$$\text{output SNR} \triangleq \frac{v_S^2}{e(S,N,H)} \tag{7}$$

By definition, the MSE is $E\{[\hat{S}(t) - S(t)]^2\}$, where $S(t)$ is the actual signal and $\hat{S}(t)$ its estimate (or output of the filter). Since $\hat{S}(t)$ can be written as $S(t) + (\hat{S}(t)-S(t))$, the error term $\hat{S}(t) - S(t)$ is considered as the noise at the output.

II. THE ε-CONTAMINATED CLASS

A. Definition

The ε-contaminated classes of possible signal and noise PSD's are defined by

$$\mathcal{S}_\varepsilon = \{S(\omega)/S(\omega) = (1-\varepsilon)S_0(\omega) + \varepsilon S'(\omega), \omega \in \mathbb{R}\} \tag{8.a}$$

and

$$\mathcal{N}_\varepsilon = \{N(\omega)/N(\omega) = (1-\varepsilon)N_0(\omega) + \varepsilon N'(\omega), \omega \in \mathbb{R}\} \tag{8.b}$$

where ε is a measure of uncertainty, $0 \le \varepsilon \le 1$, $S_0(\omega)$ and $N_0(\omega)$ are the nominal PSD's, and $S'(\omega)$ and $N'(\omega)$ are any contaminating PSD's such that

$$\int_{-\infty}^{\infty} S'(\omega)d\omega = \int_{-\infty}^{\infty} S_0(\omega)d\omega = 2\pi v_S^2 \tag{9.a}$$

and

$$\int_{-\infty}^{\infty} N'(\omega)d\omega = \int_{-\infty}^{\infty} N_0(\omega)d\omega = 2\pi v_N^2 \tag{9.b}$$

This model is reasonable for describing classes of possible PSD's which deviate to a certain extent from the nominal PSD's, subject to the total power being a constant. This general type of classes has been studied as uncertainty models in a number of situations (see [2],[4],[5],[6]).

B. Robust Filters for the ε-Contaminated Class

1. The ideal robust filter

As discussed in the introduction, a most robust filter as defined by Poor [1] is a solution to the minimax problem in (6). Its design can be shown to be reduced to the problem of finding "least-favorable" pairs of spectra S_L and N_L for which the minimum MSE is maximum in the classes $\mathcal{S}$ and $\mathcal{N}$. Then, the robust filter is simply the Wiener filter for the pair (S_L, N_L), i.e.,

$$H_R(\omega) = \frac{S_L(\omega)}{S_L(\omega) + N_L(\omega)} \tag{10}$$

It is possible to draw an analogy between least-favorable pairs of spectra and least-favorable pairs of probability density functions (PDF's) in robust hypothesis testing (see Poor [1]). Since least-favorable pairs of PDF's have been derived for several classes of PDF's (see [4],[7],[8]), this analogy can be used to determine $S_L(\omega)$ and $N_L(\omega)$ (and hence the robust filter H_R given in (10)) for analogous classes of PSD's. For example, by applying the results of Poor [1] and using the expression for least-favorable PDF's for the ε-contaminated class given by Huber[4], Vastola [3] has shown that the robust filter for the classes $\mathcal{J}_\varepsilon$ and $\mathcal{N}_\varepsilon$ is

$$H_R(\omega) = \begin{cases} k_1 \triangleq \dfrac{c_1 r}{c_1 r + 1} & \text{for } H_0^*(\omega) \leq k_1 \\[2mm] H_0^*(\omega) & \text{for } k_1 < H_0^*(\omega) < k_2 \\[2mm] k_2 \triangleq \dfrac{c_2 r}{c_2 r + 1} & \text{for } H_0^*(\omega) \geq k_2 \end{cases} \qquad (11)$$

The constants c_1 and c_2, $0 \leq c_1 < c_2 \leq \infty$, are determined by solving the following equations (see Huber [4] and Poor [1]):

$$(1-\varepsilon) \left[\int_{A_2} N_0(\omega) d\omega + \frac{1}{c_2} \int_{A_2^c} S_0(\omega) d\omega \right] = 1 \qquad (12.a)$$

$$(1-\varepsilon) \left[\int_{A_1^c} S_0(\omega) d\omega + c_1 \int_{A_1} N_0(\omega) d\omega \right] = 1 \qquad (12.b)$$

where the sets A_1 and A_2 are defined as follows:

$$A_1 = \{\omega \in \mathbb{R} / \frac{S_0(\omega)}{N_0(\omega)} \leq c_1 r\} \qquad (13.a)$$

$$A_2 = \{\omega \in \mathbb{R} / \frac{S_0(\omega)}{N_0(\omega)} < c_2 r\} \qquad (13.b)$$

For the nominal PSD's $S_0(\omega)$ and $N_0(\omega)$ given in (4.a) and (4.b), Equations (12.a) and (12.b) become

$$\frac{1}{c_2} \tan^{-1}\left(\frac{\omega_2}{a_S}\right) - \tan^{-1}\left(\frac{\omega_2}{a_N}\right) = \frac{\epsilon}{1-\epsilon} \frac{\pi}{2} \tag{14.a}$$

$$\frac{2}{\pi} \tan^{-1}\left(\frac{\omega_1}{a_S}\right) + c_1\left(1 - \frac{2}{\pi} \tan^{-1}\left(\frac{\omega_1}{a_N}\right)\right) = \frac{1}{1-\epsilon} \tag{14.b}$$

where

$$\omega_i = \left[a_N a_S\left(\frac{c_i a_S - a_N}{a_S - c_i a_N}\right)\right]^{\frac{1}{2}} \quad , \quad i = 1,2 \tag{15}$$

are the frequencies at which $H_0^*(\omega_i) = k_i$, i=1,2. For a given ϵ, $0 \leq \epsilon \leq 1$, the above equations are solved by iteration for c_1 and c_2. In particular, for the values of ϵ we will consider, we have: for $\epsilon = 0.1$, $c_1 = 0.125$ and $c_2 = 8$; for $\epsilon = 0.25$, $c_1 = 1/2.8 = 0.357$, and $c_2 = 2.8$.

Figure 1 illustrates the general frequency response of the ideal robust filter H_R, given the nominal filter H_0^*. Note that only the portions of $H_R(\omega)$ and $H_0^*(\omega)$ for positive frequencies ω are shown, since $H_R(\omega)$ and $H_0^*(\omega)$ are both symmetric with respect to the $\omega = 0$ axis.

2. The approximate robust filter

To approximate the ideal robust filter transfer function shown in Fig. 1, we will use analog Butterworth filters. These filters can be physically realized with an active network (see Van Valkenburg [9]). A low-pass n-th order Butterworth filter is characterized by the square of the magnitude of its frequency response,

$$\left|H_{Bn}(\omega)\right|^2 = \frac{1}{1+(\omega/\omega_c)^{2n}} \tag{16}$$
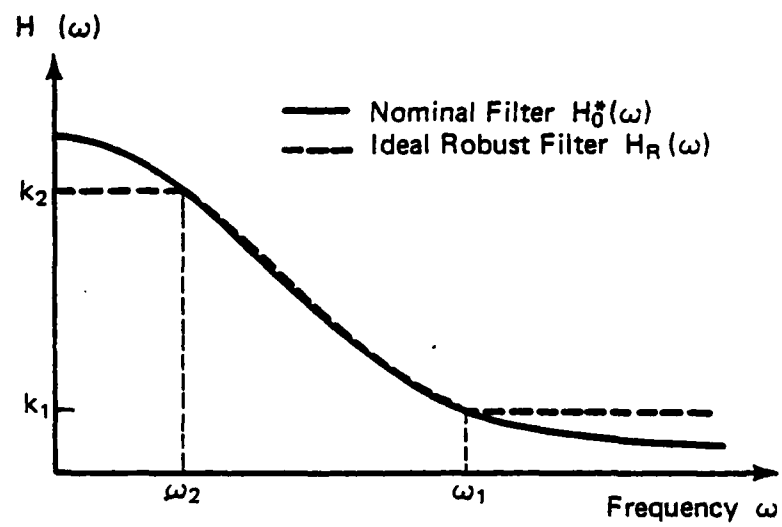
Figure 1. Nominal and ideal robust filters for the
ε-contaminated class.

where ω_c is the 3 dB cutoff frequency. The actual transfer function of a low-pass Butterworth filter can be determined by

$$H_{Bn}(j\omega) = \frac{1}{B_n(s)} \Bigg|_{s=j\frac{\omega}{\omega_c}} \tag{17}$$

where the polynomials $B_n(s)$ of degrees $n = 1,2,\ldots,10$ are tabulated Butterworth polynomials (see [9]). Figure 2 shows the magnitude squared response $|H_{Bn}(\omega)|^2$ of low-pass Butterworth filters for several orders n and $\omega_c = 1$. It can be seen that, as the order n increases, the response approaches that of the ideal low-pass filter.

The ideal robust filter as given by (11) is a non causal filter. On the other hand, Butterworth filters are causal. Therefore, in order to have an adequate comparison between the ideal and approximate robust filters, we will use, as non causal filters, the magnitude squared response of the Butterworth filters in our approximation. It should be noted that these filters $|H_{Bn}(\omega)|^2$ can be implemented (although not in real-time) by signal processing techniques (see Appendix A).

From the expression of the ideal robust filter (Eq. (11)) and Fig. 1, it is clear that we can approximate the transfer function of the ideal robust filter with three sections: the first section is realized by a low-pass filter with gain k_2 and cutoff ω_2, the last section by a high-pass filter with gain k_1 and cutoff ω_1, and the middle section by the product of the nominal filter $H_0^*(\omega)$ and a bandpass filter of unit gain and bandwidth $[\omega_2,\omega_1]$. The sum of those three sections constitutes the approximate robust filter transfer function $H_n(\omega)$, which is shown in Fig. 3. The filters $H_{LP_1}(\omega)$ and $H_{LP_2}(\omega)$ represent the magnitude squared of low-pass Butterworth filters with cutoffs ω_1 and ω_2 respectively, i.e.,
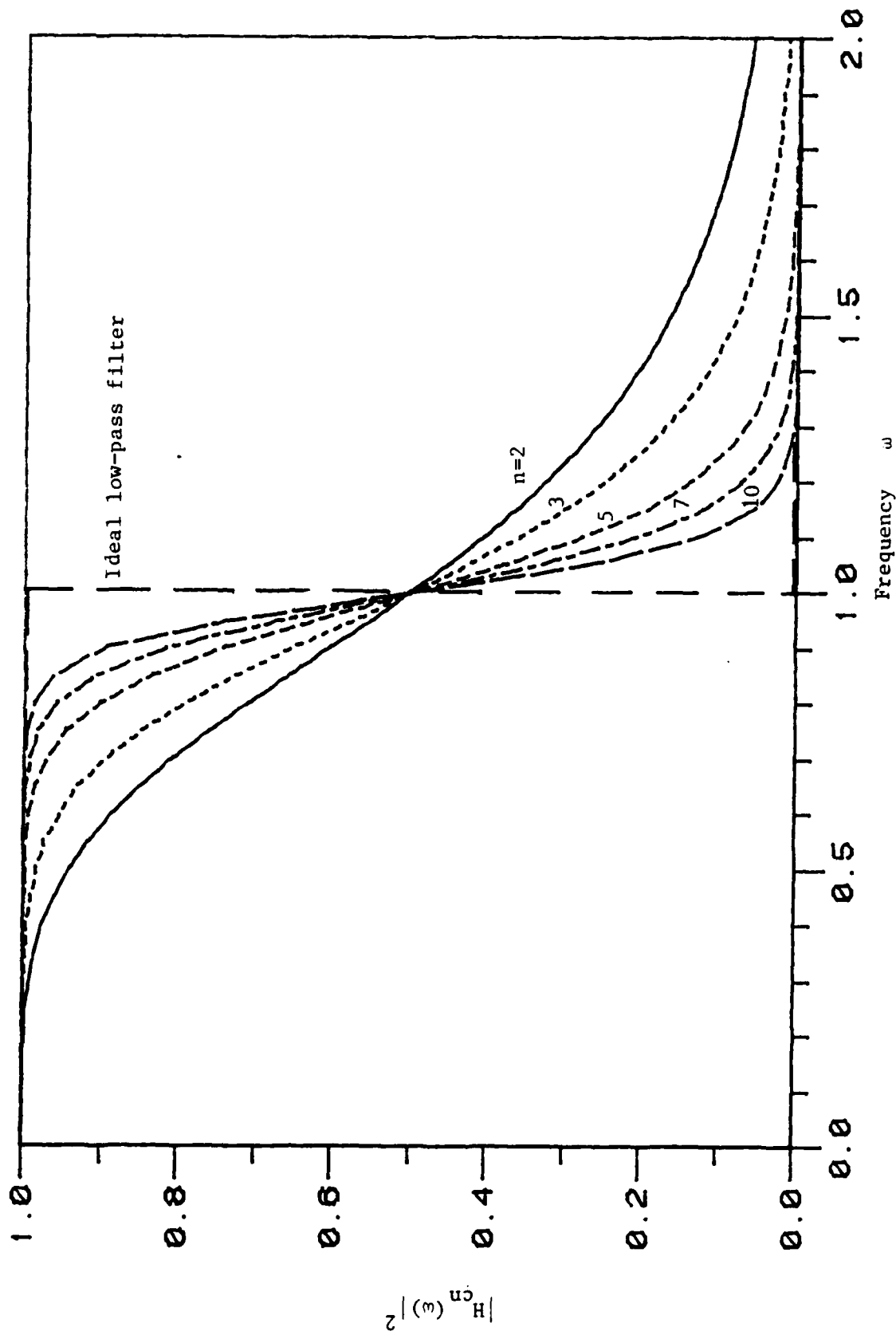
Figure 2. Magnitude squared response of n-th order low-pass Butterworth filters ($\omega_c = 1$).
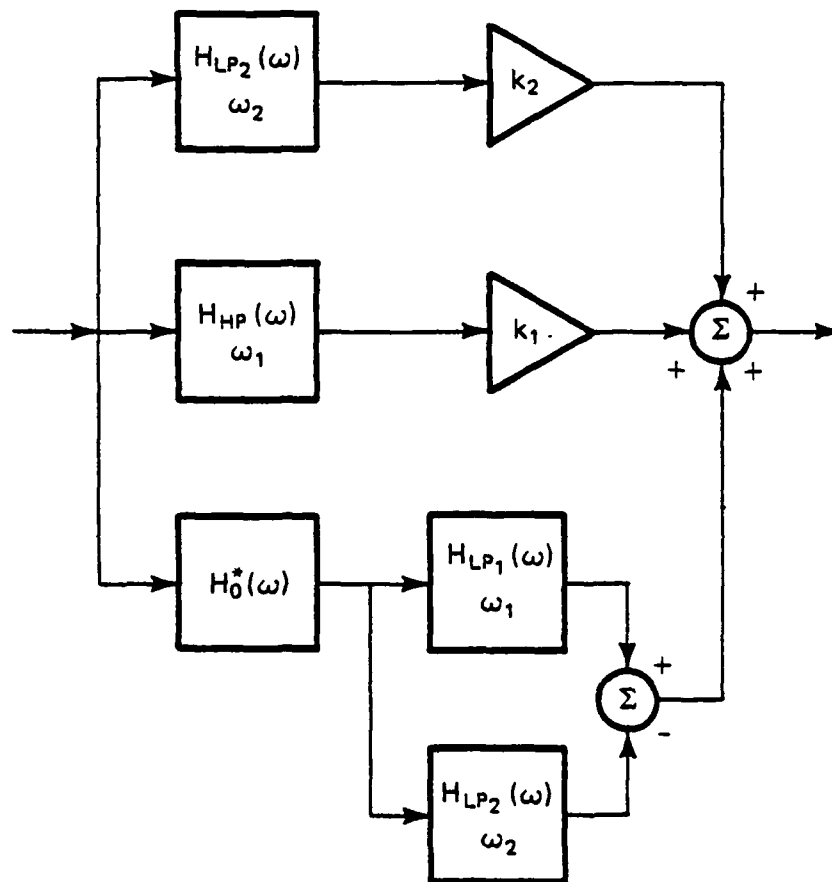
Figure 3.   Block diagram for the approximate robust
            filter $H_n(\omega)$ for the ε-contaminated class
            using Butterworth filters.

$$H_{LP_1}(\omega) = \frac{1}{1+(\omega/\omega_1)^{2n}} \tag{18}$$

and

$$H_{LP_2}(\omega) = \frac{1}{1+(\omega/\omega_2)^{2n}} \tag{19}$$

The difference $(H_{LP_1}(\omega) - H_{LP_2}(\omega))$ is used to obtain the bandpass filter of bandwidth $[\omega_2,\omega_1]$ in the middle section. The filter $H_{HP}(\omega)$ represents the magnitude squared of a high-pass Butterworth filter with cutoff ω_1, i.e.,

$$H_{HP}(\omega) = \frac{1}{1+(\omega_1/\omega)^{2n}} \tag{20}$$

From Fig. 3, we see that the resulting approximate robust filter for the ε-contaminated class is given by

$$H_n(\omega) = k_2 H_{LP_2}(\omega) + k_1 H_{HP}(\omega) + H_0^*(\omega)[H_{LP_1}(\omega) - H_{LP_2}(\omega)] \tag{21}$$

where $H_0^*(\omega)$ is the nominal filter in (5).

C. Worst-Case Performance Evaluation

In this section, our goal is to evaluate the worst-case performances of the nominal filter H_0^*, the ideal robust filter H_R, and its approximation H_n, proposed in the previous section. Performance will be measured by the output SNR as defined in the Introduction by Eq. (7). In the worst-case, we will look at the maximum MSE over all possible spectra in the relevant ε-contaminated class.

Using the general expression of the MSE (Eq. (1)) for a given pair of spectra (S,N) in the ε-contaminated class $\mathcal{J}_\varepsilon \times \mathcal{N}_\varepsilon$ (Eqs. (8.a),(8.b)), and a given filter H, it is straightforward to show that

$$e(S,N,H) = (1-\varepsilon)e(S_0,N_0,H) + \varepsilon e(S',N',H) \qquad (22)$$

We observe that the MSE expression in (22) is analogous to the expression for the ε-contaminated spectra, in the way the uncertainty is modeled. Indeed, the term $e(S',N',H)$, which is the MSE associated with the contaminating PSD's S' and N', is not known since the only information about S' and N' is their total powers. However, we can obtain an upper bound on $e(S',N',H)$ using this information, i.e.,

$$e(S',N',H) = \frac{1}{2\pi} \int_{-\infty}^{\infty} [S'(\omega)|1-H(\omega)|^2 + N'(\omega)|H(\omega)|^2]d\omega$$

$$\leq \frac{1}{2\pi} \left\{ \left[\int_{-\infty}^{\infty} S'(\omega)d\omega \right] \max_{\omega} |1-H(\omega)|^2 + \left[\int_{-\infty}^{\infty} N'(\omega)d\omega \right] \max_{\omega} |H(\omega)|^2 \right\}$$

$$= v_S^2 \max_{\omega} |1-H(\omega)|^2 + v_N^2 \max_{\omega} |H(\omega)|^2 \qquad (23)$$

The last step is true from Eqs. (9.a) and (9.b).

In fact $e(S',N',H)$ can be arbitrarily close to the bound in (23). Therefore, (23) is the least upper bound and so the worst-case performance for H is

$$\sup_{\substack{\mathscr{S}_\varepsilon \times \mathscr{N}_\varepsilon}} e(S,N,H) = (1-\varepsilon)e(S_0,N_0,H) + \varepsilon \sup_{\substack{\mathscr{S}_\varepsilon \times \mathscr{N}_\varepsilon}} e(S',N',H)$$

$$= (1-\varepsilon)e(S_0,N_0,H) + \varepsilon \left[v_S^2 \max_{\omega} |1-H(\omega)|^2 + v_N^2 \max_{\omega} |H(\omega)|^2 \right] \qquad (24)$$

To obtain the worst-case output SNR, we simply divide through Eq. (24) by the signal power v_S^2 and then take the inverse of the result. In this way, we can derive the expressions for $\sup_{\mathcal{J}_\epsilon \times \mathcal{N}_\epsilon} e(S,N,H)/v_S^2$ for H_0^*, H_R and H_n; These will be in terms of the input SNR $r = v_S^2/v_N^2$.

1. <u>Nominal filter</u>

For the nominal filter H_0^*, we have (from Eq. (3))

$$\frac{e(S_0,N_0,H_0^*)}{v_S^2} = \frac{1}{2\pi v_S^2} \int_{-\infty}^{\infty} H_0^*(\omega)N_0(\omega)\,d\omega \tag{25}$$

Using the nominal filter transfer function $H_0^*(\omega)$ given in Eq. (5) and the nominal PSD of the noise in Eq. (4.b), this reduces to

$$\frac{e(S_0,N_0,H_0^*)}{v_S^2} = \frac{2}{\pi} \int_0^{\infty} \frac{a_N a_S}{(a_N a_S)(a_S + a_N r) + (a_N + a_S r)\omega^2}\,d\omega$$

$$= \left[\frac{a_N a_S}{(a_N + a_S r)(a_S + a_N r)} \right]^{\frac{1}{2}} \tag{26}$$

Since $H_0^*(\omega)$ is a real, positive function of ω, we also have

$$\max_{\omega} |H_0^*(\omega)|^2 = \left[\max_{\omega} H_0^*(\omega) \right]^2$$

$$= \left[\frac{a_N r}{a_S + a_N r} \right] \tag{27}$$

and

$$\max_{\omega} |1-H_0^*(\omega)|^2 = \left[\max_{\omega}(1-H_0^*(\omega))\right]^2$$

$$= \left[\frac{a_N}{a_N + a_S r}\right]^2 \tag{28}$$

Therefore, using Eq. (24) for the nominal filter and the results in Eqs. (26), (27), and (28), we obtain

$$\frac{\sup\limits_{\mathcal{I}_\varepsilon \times \mathcal{N}_\varepsilon} e(S,N,H_0^*)}{v_S^2} = \left\{(1-\varepsilon)\left[\frac{a_N a_S}{(a_N+a_S r)(a_S+a_N r)}\right]^{\frac{1}{2}} \right.$$
$$\left. + \varepsilon\left[\left(\frac{a_N}{a_N+a_S r}\right)^2 + r\left(\frac{a_N}{a_S+a_N r}\right)^2\right]\right\} \tag{29}$$

2. Ideal robust filter

From the general expression for the maximum MSE for the classes $\mathcal{I}_\varepsilon$ and $\mathcal{N}_\varepsilon$ given by Eq. (24) and the ideal robust filter transfer function (see Eq. (11) and Fig. 1), we observe that the ideal robust filter H_R improves on the worst-case performance (in comparison to the nominal filter H_0^*) by decreasing the factors $\max\limits_{\omega}|H(\omega)|^2$ and $\max\limits_{\omega}|1-H(\omega)|^2$ in the worst-case MSE. This is achieved by reducing the high gain of H_0^* to a constant level k_2 over the low frequency range $[0,\omega_2]$, and increasing the low gain of H_0^* to a constant level k_1 over the high frequency range $[\omega_1,\infty)$. The constants k_1 and k_2 and the cutoff frequencies ω_1 and ω_2 depend on the degree of the uncertainty ε (see Eqs. (11),(12.a),(12.b),(14.a),(14.b),and (15)).

To evaluate the maximum MSE given in (24) for the ideal robust filter H_R, we first need to look at the nominal performance of H_R. We will break up $e(S_0,N_0,H_R)/v_S^2$ into three integral terms corresponding to the three sections constituting the ideal robust filter, i.e.,

$$\frac{e(S_0,N_0,H_R)}{v_S^2} = \frac{1}{\pi v_S^2} \int_0^\infty [S_0(\omega)|1-H_R(\omega)|^2 + N_0(\omega)|H_R(\omega)|^2]d\omega$$

$$= nsr_1 + nsr_2 + nsr_3 \qquad (30)$$

where

$$nsr_1 \stackrel{\Delta}{=} \frac{1}{\pi v_S^2} \int_0^{\omega_2} [S_0(\omega)(1-k_2)^2 + N_0(\omega)k_2^2]\, d\omega \qquad (31)$$

$$nsr_2 \stackrel{\Delta}{=} \frac{1}{\pi v_S^2} \int_{\omega_2}^{\omega_1} [S_0(\omega)|1-H_0^*(\omega)|^2 + N_0(\omega)|H_0^*(\omega)|^2]d\omega$$

$$= \frac{1}{\pi v_S^2} \int_{\omega_2}^{\omega_1} H_0^*(\omega)N_0(\omega)d\omega \qquad (32)$$

and

$$nsr_3 \stackrel{\Delta}{=} \frac{1}{\pi v_S^2} \int_{\omega_1}^\infty [S_0(\omega)(1-k_1)^2 + N_0(\omega)k_1^2]d\omega \qquad (33)$$

For the nominal pair of PSD's (S_0,N_0) given in (4.a) and (4.b), and the corresponding nominal filter H_0^* given in (5), these integrals become

$$nsr_1 = \frac{2}{\pi}\left[(1-k_2)^2 \tan^{-1}\frac{\omega_2}{a_S} + \frac{1}{r} k_2^2 \tan^{-1}\frac{\omega_2}{a_N} \right] \qquad (34)$$

$$nsr_2 = \frac{2}{\pi}\left(\frac{b}{a_S+a_N r}\right)\left[\tan^{-1}\frac{\omega_1}{b} - \tan^{-1}\frac{\omega_2}{b} \right] \qquad (35)$$

where

$$b \stackrel{\Delta}{=} \left[a_N a_S \left(\frac{a_S+a_N r}{a_N+a_S r}\right) \right]^{\frac{1}{2}} \qquad (36)$$

and

$$nsr_3 = \frac{2}{\pi}\left[(1-k_1)^2 \left(\frac{\pi}{2} - \tan^{-1}\frac{\omega_1}{a_S}\right) + \frac{1}{r} k_1^2 \left(\frac{\pi}{2} - \tan^{-1}\frac{\omega_1}{a_N}\right) \right] \qquad (37)$$

On the other hand, we have

$$\max_{\omega} \left| H_R(\omega) \right|^2 = k_2^2 \tag{38}$$

and

$$\max_{\omega} \left| 1 - H_R(\omega) \right|^2 = (1-k_1)^2 \tag{39}$$

Therefore, using Eqs. (24), (30), (34)~(39), the worst-case performance of the ideal robust filter can be determined from

$$\frac{\sup\limits_{\mathscr{S}_\epsilon \times \eta_\epsilon} e(S,N,H_R)}{v_S^2} = \left\{ (1-\epsilon)\left[\frac{2}{\pi}\left[(1-k_2)^2 \tan^{-1}\frac{\omega_2}{a_S} + \frac{1}{r} k_2^2 \tan^{-1}\frac{\omega_2}{a_N} \right.\right.\right.$$

$$+ \frac{b}{a_S + a_N r}\left(\tan^{-1}\frac{\omega_1}{b} - \tan^{-1}\frac{\omega_2}{b} \right)$$

$$+ (1-k_1)^2 \left(\frac{\pi}{2} - \tan^{-1}\frac{\omega_1}{a_S} \right)$$

$$\left.\left. + \frac{k_1^2}{r}\left(\frac{\pi}{2} - \tan^{-1}\frac{\omega_1}{a_N} \right) \right] \right]$$

$$\left. + \epsilon \left[(1-k_1)^2 + \frac{1}{r} k_2^2 \right] \right\} \tag{40}$$

For a given ϵ, the worst-case output SNR $\dfrac{v_S^2}{\sup\limits_{\mathscr{S}_\epsilon \times \eta_\epsilon} e(S,N,H_R)}$ is a function

of the parameters ω_1, ω_2, k_1, k_2, b, and r. We note that ω_1 and ω_2 are fixed (given ϵ) but k_1, k_2, and b are functions of the input SNR r.

3. Approximate robust filter

Using Eq. (24) for the approximate robust filter $H_n(\omega)$ given in Eq. (21), we have

$$\frac{\sup\limits_{\substack{\mathscr{S}\epsilon \times \eta_\epsilon}} e(S,N,H_n)}{v_S^2} = \left\{ (1-\epsilon)\; \frac{e\left(S_0,N_0,H_n\right)}{v_S^2} \right.$$

$$\left. + \epsilon\left[\max_\omega \left|1-H_n(\omega)\right|^2 + \frac{1}{r}\max_\omega \left|H_n(\omega)\right|^2 \right] \right\} \qquad (41)$$

where the integral

$$\frac{e(S_0,N_0,H_n)}{v_S^2} = \frac{2}{\pi}\int_0^\infty \left[\frac{a_S}{a_S^2+\omega^2}\;\left|1-H_n(\omega)\right|^2 + \frac{1}{r}\,\frac{a_N}{a_N^2+\omega^2}\;\left|H_n(\omega)\right|^2 \right]d\omega \qquad (42)$$

and the maxima of $\left|1-H_n(\omega)\right|^2$ and $\left|H_n(\omega)\right|^2$ are computed numerically, given the degree of uncertainty ϵ, the order n, and the input SNR r. In our numerical results, we have taken the nominal signal and noise bandwidths to be $a_S = 1$ and $a_N = 1000$, respectively.

Figures 4 and 5 illustrate the worst-case performances of the nominal filter H_0^*, and the ideal and approximate robust filters H_R and H_n (n = 2), expressed in terms of the worst-case output SNR versus the input SNR, for $\epsilon = 0.25$ and 0.1, respectively. Both SNR's are translated into dB, i.e.,

$$\text{input SNR} = 10\,\log_{10}\frac{v_S^2}{v_N^2} \qquad (43.\text{a})$$

and

$$\text{"worst-case" output SNR} = 10\,\log_{10}\left(v_S^2 \Big/ \sup_{\substack{\mathscr{S}\epsilon \times \eta_\epsilon}} e(S,N,H) \right)$$

$$= -10\,\log_{10}\left(\sup_{\substack{\mathscr{S}\epsilon \times \eta_\epsilon}} e(S,N,H) \Big/ v_S^2 \right) \qquad (43.\text{b})$$
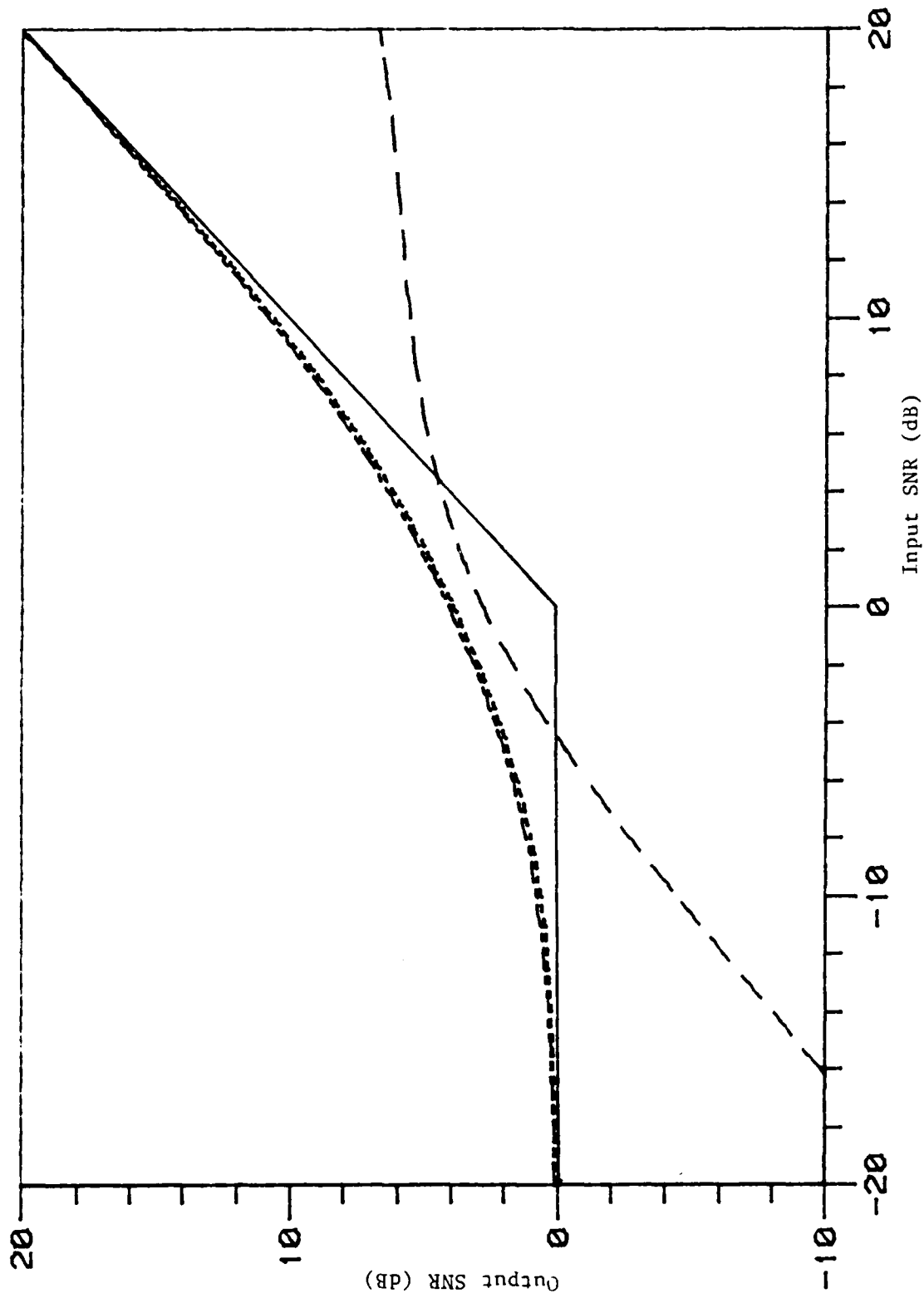
Figure 4. ε-Contaminated class ($\varepsilon = 0.25$). Butterworth approximation. (From top to bottom, except solid line) Worst-case performances of ideal robust filter H_R, approximate robust filter H_n ($n=2$), and nominal filter H_0^* (solid line is for trivial filtering).
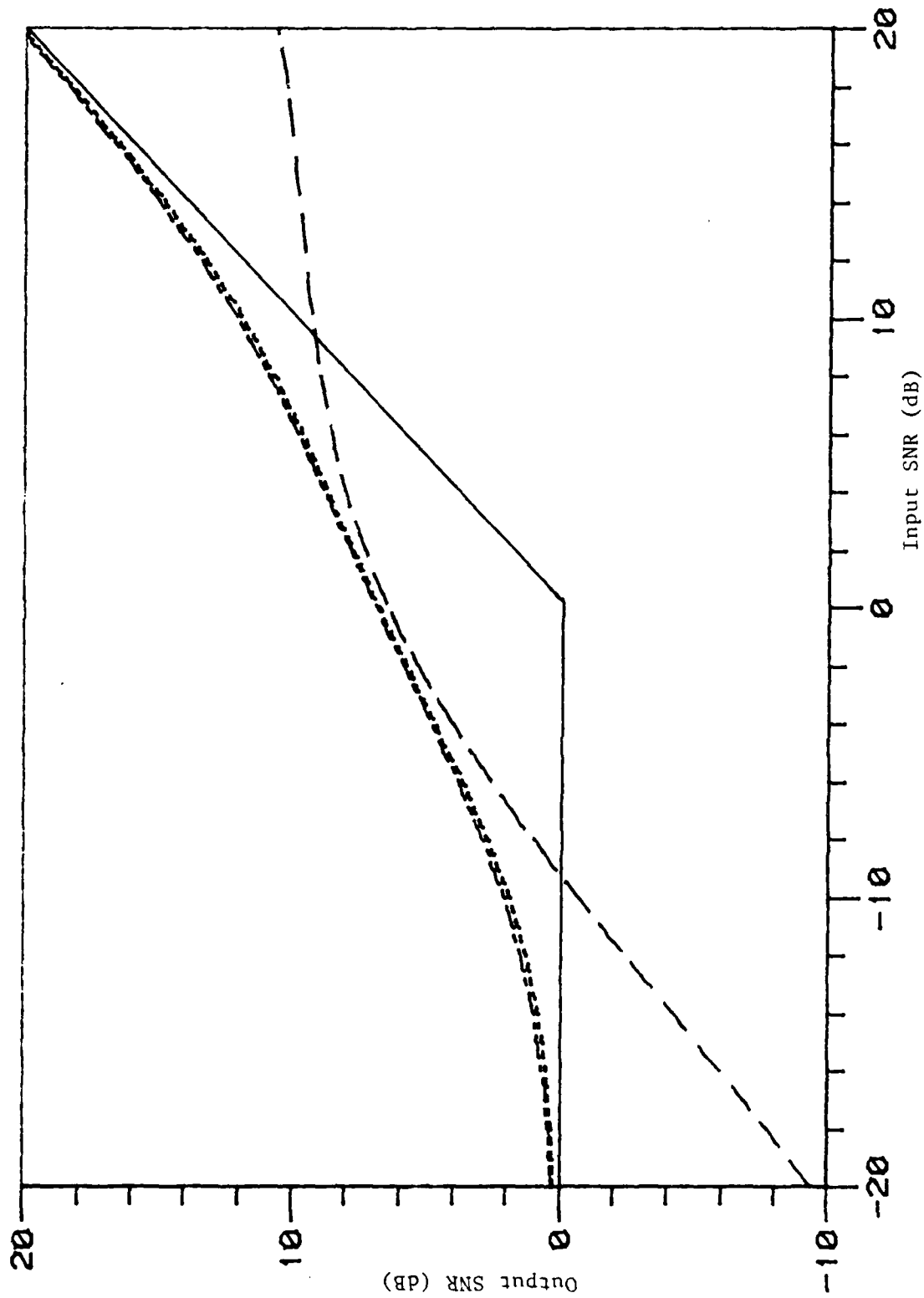
Figure 5. ε-Contaminated class (ε=0.1). Butterworth approximation. (From top to bottom, except solid line) Worst-case performances of ideal robust filter H_R, approximate robust filter H_n (n=2), and nominal filter H_0^* (solid line is for trivial filtering).

The ratio $\sup\limits_{\mathcal{J}_\varepsilon \times \mathcal{N}_\varepsilon} e(S,N,H)/v_S^2$ is given by Eqs. (29), (40) and (41) for H_0^*,

H_R and H_n, respectively. The solid line in Figs. 4 and 5 gives a lower bound on the output SNR: it represents what we can do trivially for any pair of spectra by using a no-pass filter ($H \equiv 0$) for negative input SNR's and an all-pass filter ($H \equiv 1$) for positive input SNR's. The middle and upper lines give the worst-case performances of the ideal and approximate robust filters H_R and H_n ($n = 2$), respectively. The bottom line gives the worst-case performance of the nominal filter H_0^*. We observe that, except for a small range of input SNR around 0 dB, the nominal filter does significantly worse than trivial filtering and even for values of the input SNR near 0 dB, it still does worse than both ideal and approximate robust filters. From our numerical results, we found that the worst-case performances of the approximate robust filters $H_n(\omega)$ for $n = 2$ to 10 improve only slightly with increased order n. Thus, we have only shown the performance of $H_2(\omega)$ in our figures, since the difference between $H_2(\omega)$ and $H_n(\omega)$ for higher n would be almost indistinguishable. However, we can see from Figs. 4 and 5 that even $H_2(\omega)$ has a performance that is sufficiently close to the ideal robust filter for both values of ε considered (less than 0.2 dB difference).

We also note that for $\varepsilon = 0.1$ (10% uncertainty), performance is better for all filters (H_0^*, H_R, and H_n) than for $\varepsilon = 0.25$ (25% uncertainty), which is to be expected since with less uncertainty, the ε-contaminated spectra are closer to the nominal spectra.

The general conclusion we can draw from these results is that, using only simple Butterworth filters of low order ($n = 2$), we have been able to obtain a very good approximation of the ideal robust filter in terms of worst-case performance over the ε-contaminated classes of spectra.

III.   THE p-POINT CLASS

A.   Definition

For this uncertainty class, we assume that the only information we have about the PSD's of the signal and noise is their total powers v_S^2 and v_N^2, and that we can estimate the fraction of these powers in some bands of the frequency domain.   Formally, the p-point spectral classes have been defined in Cimini and Kassam [10] by

$$\mathscr{S}_p = \{S(\omega) / \frac{1}{\pi} \int_{b_{j-1}}^{b_j} S(\omega) d\omega = p_{Sj} v_S^2 \quad j=1,2,\ldots,m\} \tag{44.a}$$

and

$$\mathscr{N}_p = \{N(\omega) / \frac{1}{\pi} \int_{b_{j-1}}^{b_j} N(\omega) d\omega = p_{Nj} v_N^2 \quad j=1,2,\ldots,m\} \tag{44.b}$$

where $b_0, b_1, \ldots, b_m$ are $m+1$ breakpoints on the frequency axis with $b_0 = 0$, $b_m = \infty$, and $0 \leq p_{Sj}, p_{Nj} \leq 1$ are such that $\sum_{j=1}^{m} p_{Sj} = \sum_{j=1}^{m} p_{Nj} = 1$, and we assume $S(\omega)$ and $N(\omega)$ are symmetric about the $\omega=0$ axis.   In this definition, the breakpoints b_j and the fractional powers $p_{Sj} v_S^2$ and $p_{Nj} v_N^2$ are assumed known.   Such a model is reasonable because it is possible to measure the fractional powers of a process.

A simple example of a p-point class that has been considered by Vastola [3] is one with three breakpoints (m=2), where $b_0 = 0$, $b_1 = 1$ and $b_2 = +\infty$.

B.   Robust Filters for the p-Point Class

1.   The ideal robust filter

By expressing the ideal robust filter $H_R(\omega)$ in terms of the least-favorable pair of PSD's $S_L(\omega)$ and $N_L(\omega)$ (see Eq. (10)) for the p-point spectral class, Cimini and Kassam have shown that $H_R(\omega)$ is a piecewise constant filter given by

$$H_R(\omega) = \left\{ \frac{P_{Sj} \, v_S^2}{P_{Sj} \, v_S^2 + P_{Nj} \, v_N^2} \triangleq K_{rj} \, , \quad \begin{array}{l} \omega \in [\, b_{j-1}, \, b_j) \\ j = 1, \ldots, m \end{array} \right. \tag{45}$$

with $H_R(\omega)$ symmetric about the $\omega=0$ axis. For the special case of m=2 and $b_0 = 0$, $b_1 = 1$, $b_2 = +\infty$, considered by Vastola [3], the ideal robust filter is simply

$$H_R(\omega) = \left\{ \begin{array}{ll} \dfrac{P_{S1} \, v_S^2}{P_{S1} \, v_S^2 + P_{N1} \, v_N^2} \triangleq K_{r1} \, , & \omega \in [\, 0, \, 1) \\[4ex] \dfrac{(1-P_{S1}) v_S^2}{(1-P_{S1}) v_S^2 + (1-P_{N1}) v_N^2} \triangleq K_{r2} \, , & \omega \in [\, 1, \, \infty) \end{array} \right. \tag{46}$$

and is shown in Fig. 6.

In this study, we will slightly modify the above special case by introducing a small intermediate region around $\omega=1$. In particular, the p-point class we will consider has four breakpoints (m=3) at $b_0 = 0$, $b_1 = 1-a$, $b_2 = 1+a$, and $b_3 = +\infty$, where the parameter a, $0 \le a \le 0.4$, will be chosen to optimize the output SNR for the approximate robust filter H_n for a given order n and a given input SNR. The corresponding ideal robust filter $H_R(\omega)$ is shown in Fig. 7 where the gains K_{rj}, j=1,2,3, are given by Eq. (45). Note that for a=0, this filter reduces to the m=2 case with $b_0 = 0$, $b_1 = 1$, and $b_2 = +\infty$.

The reasons for using this modification lie in the general expression of the maximum MSE for the p-point class and in the structure of the approximate robust filters that will be used. A more detailed explanation is given in Appendix B, as well as the procedure for choosing the parameter a.
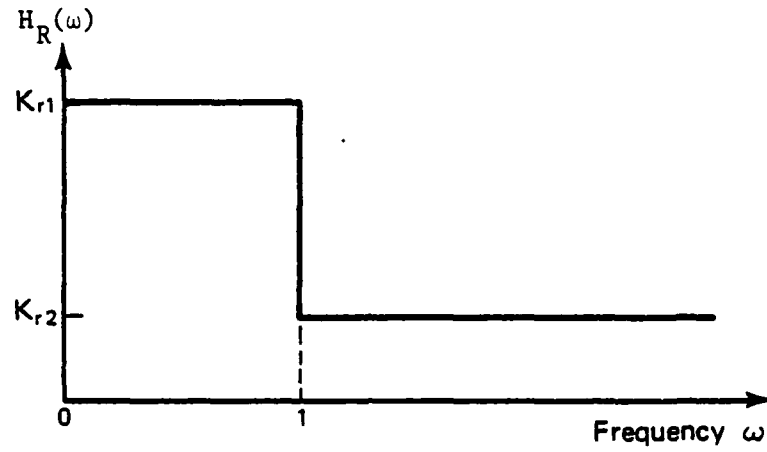
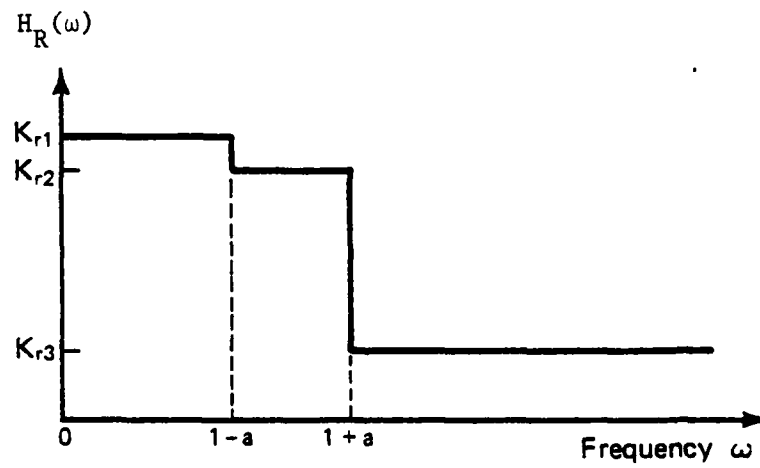Figure 6.   Ideal robust filter for the p-point class with $m = 2$, $b_0 = 0$, $b_1 = 1$, and $b_2 = +\infty$.

Figure 7.   Ideal robust filter for the p-point class with $m = 3$, $b_0 = 0$, $b_1 = 1-a$, $b_2 = 1+a$, and $b_3 = +\infty$.

2. Approximate robust filters

To approximate the ideal robust filter shown in Fig. 7, we will sum up the response of a low-pass filter with cutoff $\omega_c = 1$ and gain $K_1 = K_{r1} - K_{r3}$ with the response of an all-pass filter with gain $K_2 = K_{r3}$, as shown in Fig. 8, i.e., the approximate robust filter can be expressed as

$$H_n(\omega) = K_1 H_{LP}(\omega) + K_2 \tag{47}$$

The low-pass filter with unit gain $H_{LP}(\omega)$ will be realized using either an analog Butterworth or Chebyshev low-pass filter. A brief description on analog Butterworth filters was given in Chapter II, Section B.2. Analog Chebyshev filters can also be realized with an active network (see [9]). A low-pass n-th order Chebyshev filter has equal ripple behavior in the pass-band, and the square of the magnitude of its frequency response is given by

$$\left| H_{Cn}(\omega) \right|^2 = \frac{1}{1 + \beta^2 C_n^2(\omega)} \tag{48}$$

where

$$C_n(\omega) = \begin{cases} \cos\,(n \cos^{-1} \omega), & |\omega| \le 1 \\ \cosh\,(n \cosh^{-1} \omega), & |\omega| > 1 \end{cases} \tag{49}$$

is known as the Chebyshev polynomial of the first kind of degree n, and the peak-to-peak ripple γ in dB in the passband is

$$\gamma = 10 \log_{10}\,(1 + \beta^2) \tag{50}$$

The minimum and maximum values of the ripple are $1/(1 + \beta^2)$ and 1, respectively, and the number of half cycles in the passband ripple is equal to the order n of the filter. In general, the magnitude response of the filters with even
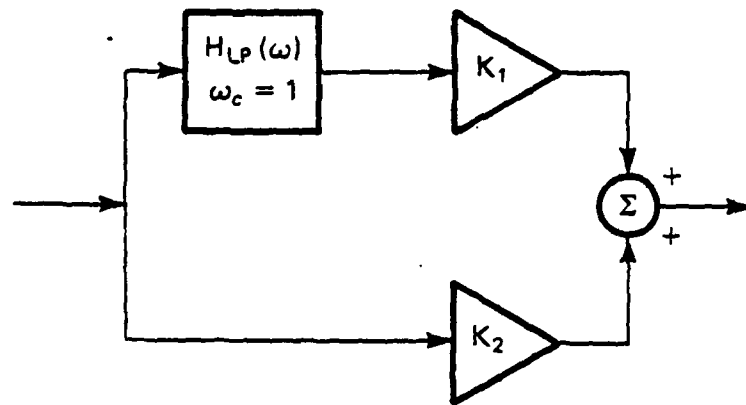
Figure 8. Block diagram for the approximate robust
filter $H_n(\omega)$ for the p-point class.

orders n at $\omega=0$ is equal to the minimum value of the ripple while that of the filters with odd order n is equal to the maximum value of the ripple, but the response for all filters passes through the same point at the edge of the passband (i.e., at $\omega_c = 1$) which corresponds to the minimum value of the ripple. Figures 9(a), 9(b), and 9(c) illustrate the magnitude squared response of n-th order low-pass Chebyshev filters for ripples $\gamma = 0.5$, 1, and 2 dB, respectively. We observe that, for a given order n, the larger the ripple γ, the steeper the rolloff in the stopband. This effect is more accentuated for small values of n. Furthermore, by comparing the magnitude squared responses of low-pass Chebyshev and Butterworth filters (see Figs. 9(a), 9(b), 9(c), and 2), we see that, in general, the Chebyshev response has steeper rolloffs in the stopband than the Butterworth response, and for orders $n \geq 4$, Chebyshev filters have larger attenuations near the cutoff frequency $\omega_c = 1$ in the stopband. However, like Butterworth filters, they are rational functions, since the transfer function of a low-pass Chebyshev filter is

$$H_{Cn}(\omega) = \frac{1}{\beta 2^{n-1} Q_n(\omega)} \tag{51}$$

where $Q_n(\omega)$, $n = 2,\ldots,10$ are tabulated polynomials of degree n (see Craig [11]). The procedure for finding the poles of the above transfer function is also found in Van Valkenburg [9].

For reasons of causality (as discussed in Chapter II, Section B.2), we will actually use the magnitude squared of the Butterworth or Chebyshev low-pass filters in our approximation. Therefore, for the Butterworth case, the approximate robust filter is

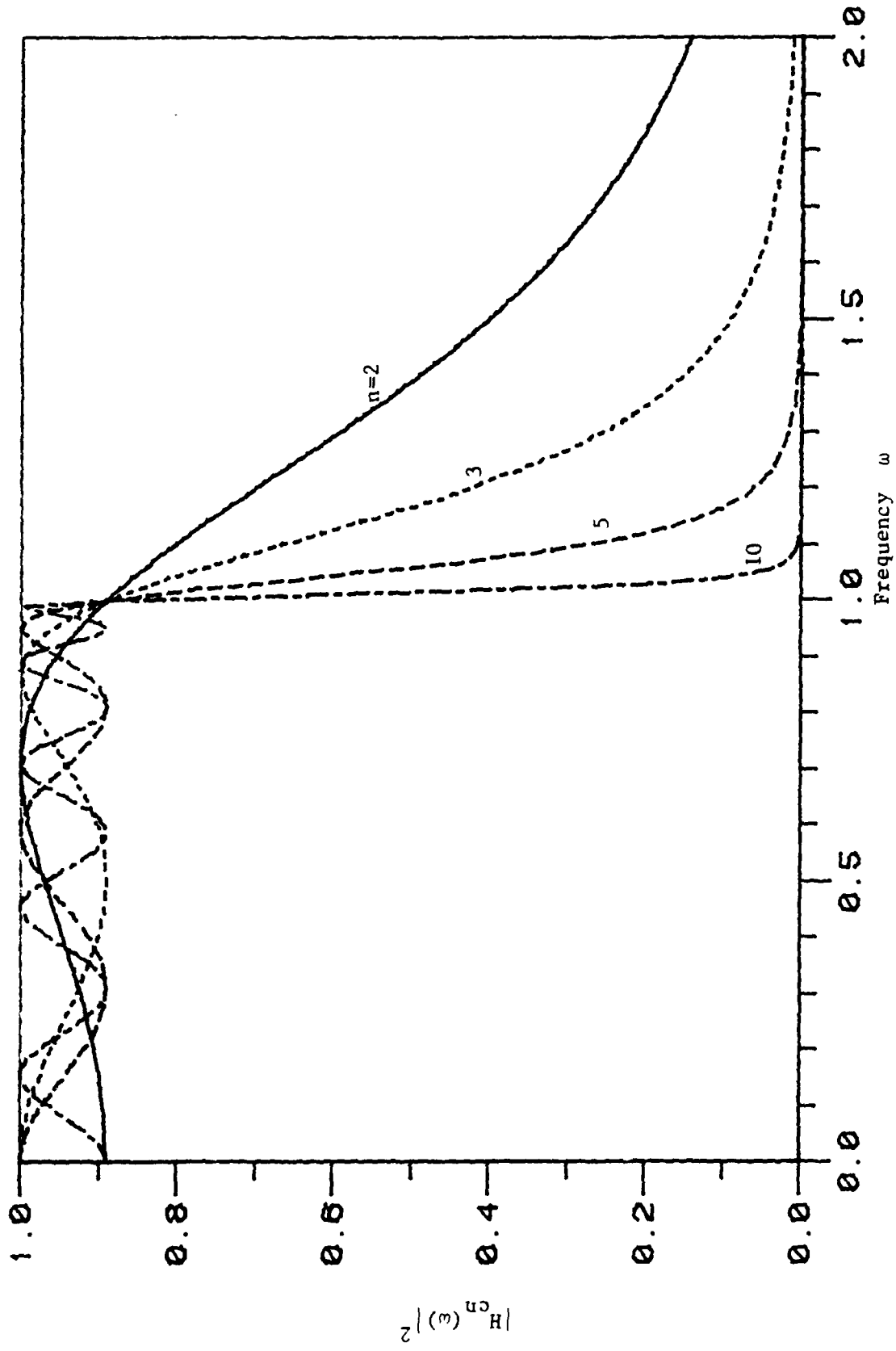$$H_n(\omega) = K_{1B} |H_{Bn}(\omega)|^2 + K_{2B} \tag{52}$$

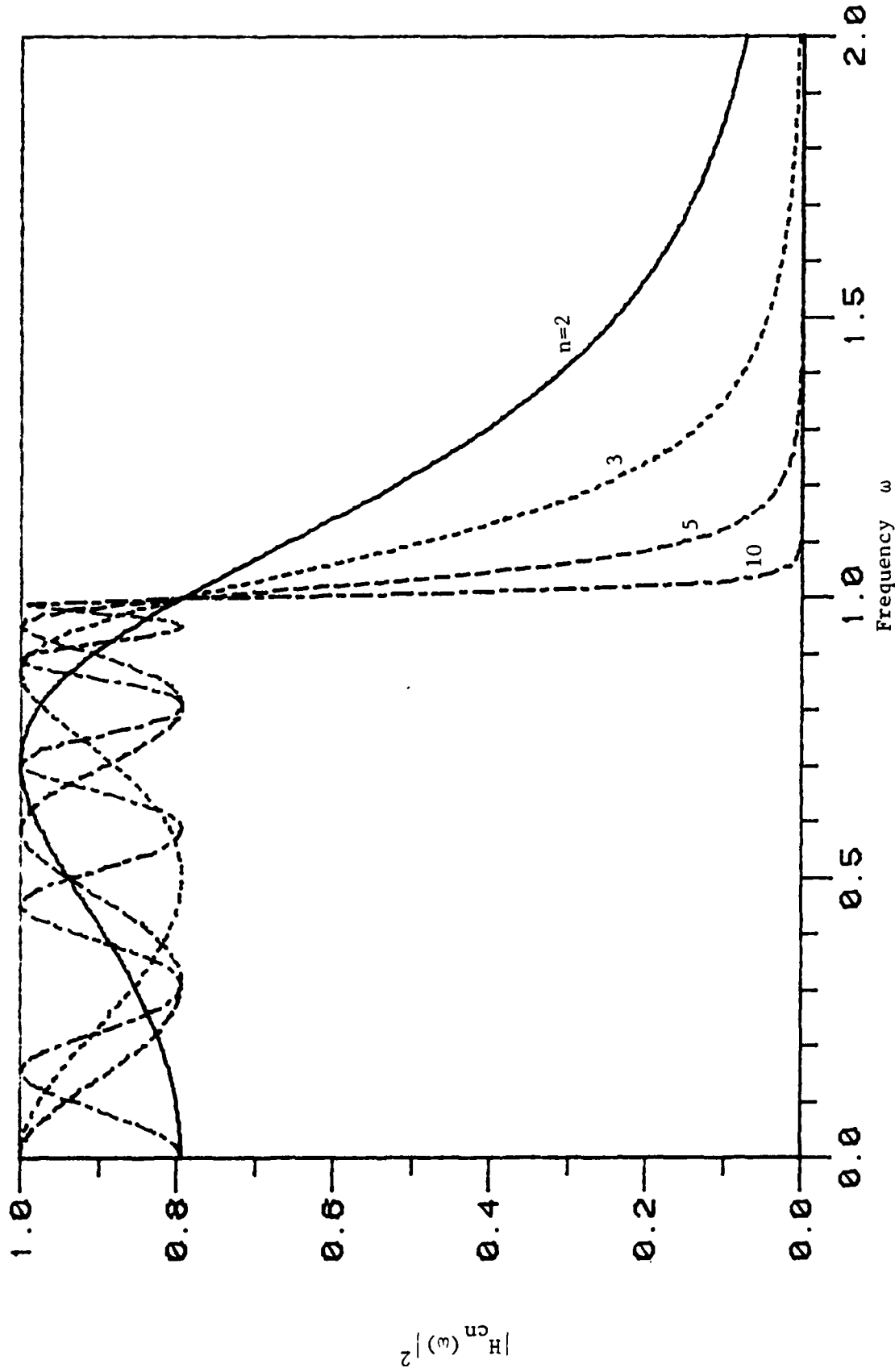Figure 9(a). Magnitude squared response of the n-th order low-pass Chebyshev filters. (ripple $\gamma = 0.5$dB)

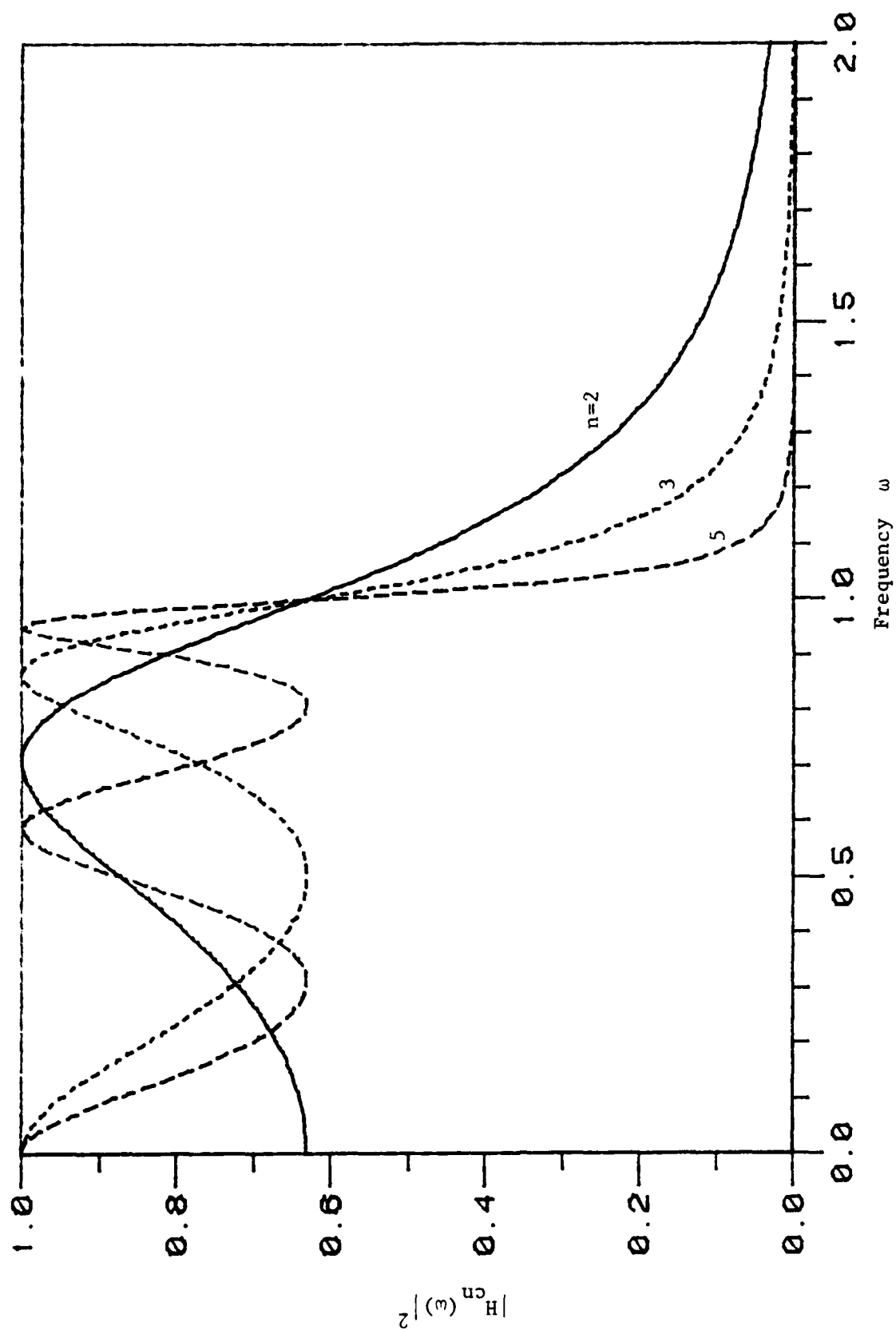Figure 9(b). Magnitude squared response of n-th order low-pass Chebyshev filters. ($\gamma = 1dB$)

Figure 9(c). Magnitude squared response of the n-th order low-pass Chebyshev filters (γ=2dB)

where $|H_{Bn}(\omega)|^2$ is given by Eq. (16) with $\omega_c = 1$ and $K_{1B} = K_{r1} - K_{r3}$, $K_{2B} = K_{r3}$ to match the ideal robust filter gains. For the Chebyshev case, the approximate robust filter is

$$H_n(\omega) = K_{1C}|H_{Cn}(\omega)|^2 + K_{2C} \tag{53}$$

where $|H_{Cn}(\omega)|^2$ is given by Eq. (48). Here, the gain $K_{2C} = K_{r3}$, as for the Butterworth approximation, but the gain K_{1C} is

$$K_{1C} = (K_{r1} - K_{r3})K_S \tag{54}$$

where K_S is a scale factor such that the Chebyshev ripple in Figs. 9(a), 9(b), and 9(c) is centered about a gain of 1 (instead of having its maxima at 1). It is easy to show that

$$K_S = \frac{2(1 + \beta^2)}{2 + \beta^2} \tag{55}$$

C. Worst-Case Performance Evaluation

As for the ε-contaminated class, we will look at the worst-case performance of the nominal filter and the ideal and approximate robust filters by evaluating the worst-case output SNR as given by Eq. (43.b) (with the ε-contaminated classes $\mathscr{J}_\varepsilon$ and $\mathcal{N}_\varepsilon$ replaced by the p-point classes $\mathscr{J}_p$ and $\mathcal{N}_p$). Therefore, we would like to derive expressions for $\displaystyle\sup_{(S,N) \in \mathscr{J}_p \times \mathcal{N}_p} e(S,N,H)/v_S^2$ for the different filters considered.

Since the only knowledge about the PSD's $S(\omega)$ and $N(\omega)$ in the p-point class is their total and fractional powers, we can use this information to obtain an upper bound on the MSE. To do this, the integral in the MSE expression, as given by Eq. (1), is broken up into the three intervals $[b_0, b_1)$, $[b_1, b_2)$, and $[b_2, b_3)$ where $b_0 = 0$, $b_1 = 1-a$, $b_2 = 1+a$, and $b_3 = \infty$, i.e.,

$$e(S,N,H) = \frac{1}{\pi} \sum_{j=1}^{3} \int_{b_{j-1}}^{b_j} [S(\omega)|1-H(\omega)|^2 + N(\omega)|H(\omega)|^2] d\omega$$

$$\leq \frac{1}{\pi} \sum_{j=1}^{3} \left\{ \left[\int_{b_{j-1}}^{b_j} S(\omega)d\omega \right] \max_{\omega \in [b_{j-1}, b_j)} |1-H(\omega)|^2 \right.$$

$$\left. + \left[\int_{b_{j-1}}^{b_j} N(\omega)d\omega \right] \max_{\omega \in [b_{j-1}, b_j)} |H(\omega)|^2 \right\}$$

$$= \sum_{j=1}^{3} \left\{ P_{Sj} v_S^2 \max_{\omega \in I_j} |1-H(\omega)|^2 + P_{Nj} v_N^2 \max_{\omega \in I_j} |H(\omega)|^2 \right\}$$

where (56)

$$I_j \triangleq [b_{j-1}, b_j). \tag{57}$$

The last step is true from the definition of the p-point spectral classes (see Eqs. (44.a), (44.b)).

In fact, the bound in (56) is the least upper bound on e(S,N,H). Therefore, the worst-case performance for H is

$$\sup_{\mathscr{S}_p \times \mathcal{N}_p} e(S,N,H) = \sum_{j=1}^{3} \left\{ P_{Sj} v_S^2 \max_{\omega \in I_j} |1-H(\omega)|^2 + P_{Nj} v_N^2 \max_{\omega \in I_j} |H(\omega)|^2 \right\}$$

$$\tag{58}$$

Note that the fractions P_{Sj} and P_{Nj} can be found from (see Eqs. (44.a) and (44.b))

$$P_{Sj} = \frac{1}{\pi v_S^2} \int_{b_{j-1}}^{b_j} S_0(\omega)d\omega$$

$$= \frac{2}{\pi} \left[\tan^{-1} \frac{b_j}{a_S} - \tan^{-1} \frac{b_{j-1}}{a_S} \right], \quad j=1,2,3 \tag{59.a}$$

and

$$P_{Nj} = \frac{1}{\pi v_N^2} \int_{b_{j-1}}^{b_j} N_0(\omega) d\omega$$

$$= \frac{2}{\pi} \left[\tan^{-1} \frac{b_j}{a_N} - \tan^{-1} \frac{b_{j-1}}{a_N} \right] , \quad j=1,2,3 \tag{59.b}$$

where $S_0(\omega)$ and $N_0(\omega)$ are the nominal densities (given by Eqs. (4.a) and (4.b)) which we assume to be the true spectra.

1. Nominal filter

Since the nominal filter $H_0^*(\omega)$ given by Eq. (5) is a real, continuous, monotone decreasing function of ω and $0 < H_0^*(\omega) \leq 1$, we have

$$\max_{\omega \in [b_{j-1}, b_j)} |H_0^*(\omega)|^2 = [H_0^*(\omega = b_{j-1})]^2, \quad j=1,2,3 \tag{60.a}$$

and

$$\max_{\omega \in [b_{j-1}, b_j)} |1-H_0^*(\omega)|^2 = [1-H_0^*(\omega = b_j)]^2, \quad j=1,2,3 \tag{60.b}$$

where $b_0 = 0$, $b_1 = 1-a$, $b_2 = 1+a$, and $b_3 = +\infty$. The above maxima can easily be computed using Eq. (5) and then substituted in Eq. (58). The results for the special case a=0 can be found in Vastola [3] and show that the performance of the nominal filter H_0^* is unacceptable since it is significantly worse than trivial filtering.

2. Ideal robust filter

For the ideal robust filter H_R considered (see Fig. 6 and Eq. (45)), it is easy to show (using Eq. (58)) that

$$\frac{\sup_{\mathcal{J}_p \times \mathcal{N}_p} e(S,N,H_R)}{v_S^2} = \sum_{j=1}^{3} \frac{p_{Sj} \; p_{Nj}}{p_{Sj}r + n_{\cdot}} \tag{61}$$

where the fractions p_{Sj} and p_{Nj} are given in Eqs. (59.a) and (59.b).

3. Approximate robust filter with Butterworth approximation

Using Eq. (58) for the approximate robust filter $H_n(\omega)$ given by Eq. (52) for the Butterworth case, we have

$$\frac{\sup_{\mathcal{J}_p \times \mathcal{N}_p} e(S,N,H_n)}{v_S^2} = \sum_{j=1}^{3} p_{Sj} \max_{\omega \in I_j} \left|1-H_n(\omega)\right|^2 + p_{Nj} \frac{\max_{\omega \in I_j} \left|H_n(\omega)\right|^2}{r} \tag{62}$$

with $I_1 = [\,0,\ 1-a)$, $I_2 = [\,1-a,\ 1+a)$, and $I_3 = [\,1+a,\ \infty)$. The optimal value of the parameter a, $0 \le a \le 0.4$, is determined for each order n, as discussed in Appendix B. Since the Butterworth magnitude squared response $\left|H_{Bn}(\omega)\right|^2$ is a real, monotone decreasing function of ω, and the gains K_{rj} of the ideal robust filter are such that $0 < K_{rj} < 1$, the maxima in Eq. (62) are easily evaluated, i.e.,

$$\max_{\omega \in I_j} \left|H_n(\omega)\right|^2 = (H_n(\omega = b_{j-1}))^2, \quad j=1,2,3 \tag{63.a}$$

and

$$\max_{\omega \in I_j} \left|1-H_n(\omega)\right|^2 = (1-H_n(\omega = b_j))^2, \quad j=1,2,3 \tag{63.b}$$

As for the ε-contaminated class, we have presented the numerical results in terms of worst-case output SNR versus input SNR, both expressed in dB (see Eqs. (43.a) and (43.b)). The ratio $\sup_{\mathcal{J}_p \times \mathcal{N}_p} e(S,N,H)/v_S^2$ is given by Eqs. (61) and (62) for the ideal robust filter H_R and the approximate robust filter

H_n, respectively. As is shown in Appendix B, we will use a value of a=0 for the ideal robust filter because its performance is relatively insensitive to variations of the parameter a, and the optimal value of a corresponding to each approximate robust filter H_n, n=2,3,...,10. In our numerical results for the p-point class, we have taken the nominal signal and noise bandwidths to be a_S = 1 and a_N = 10, respectively.

Figure 10 illustrates the worst-case performances of the ideal robust filter H_R and of the approximate robust filter H_n using the Butterworth approximation. We observe that, as the order n increases, the worst-case performance of the approximate robust filters H_n gradually approaches that of the ideal robust filter H_R. The tenth order filter gives a fairly good approximation of H_R (less than 0.7 dB difference), while the second order filter does generally better than trivial filtering except for small SNR's where it does slightly worse. In general, we see that for orders n $\geq$ 4, the approximation is adequate. The improvement in performance for higher orders n is to be expected, of course, since the response of the approximate robust filter $H_n(\omega)$ becomes closer to that of the ideal robust filter $H_R(\omega)$ as n increases.

4. Approximate robust filter with Chebyshev approximation

The worst-case performance of the approximate robust filter using the Chebyshev filters is still given by Eq. (62) but with $H_n(\omega)$ of Eq. (53). In this case, the optimal value of the parameter a is determined for each order n and each value of the ripple γ considered (see Appendix B, Table 3). Furthermore, the maxima in Eq. (62) depend on the locations of the maxima of the ripple of the Chebyshev filters relative to (1-a) (see Figs. 9(a),
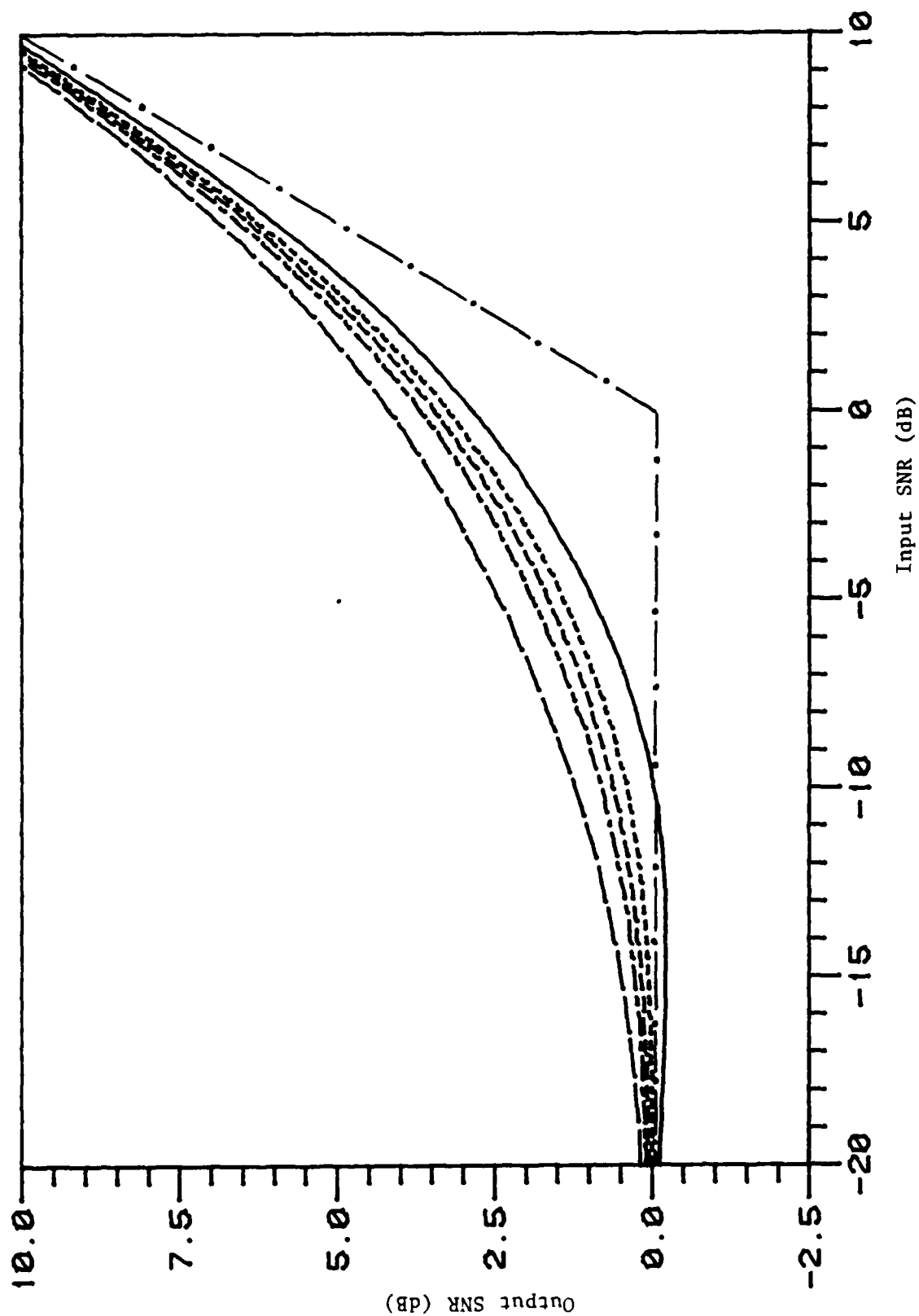
Figure 10. p-Point class. Butterworth approximation. (From top to bottom) Worst-case performances of ideal robust filter H_R, approximate robust filters H_n, n=10, 6, 4, 2, and trivial filtering.

(b), and (c)) and on the gains of the ideal robust filter. It can be shown that these maxima are

$$
\max_{\omega \in [0, 1-a)} |H_n(\omega)|^2 = \begin{cases} (K_{1C} + K_{2C})^2 & \text{if } 1-a > \omega_{max}(n, k_{max}) \\ |H_n(\omega)|^2 \big|_{\omega = 1-a} & \text{if } 1-a \leq \omega_{max}(n, k_{max}) \end{cases}
$$

where $\hspace{10cm}$ (64)

$$
\omega_{max}(n,k) = \cos\left(\frac{(2k + 1)\pi}{2n}\right), \quad k = 0,1,\ldots,k_{max}
$$

$$
\text{with } k_{max} = \begin{cases} \dfrac{n}{2} - 1, & n \text{ even} \\ \dfrac{n-1}{2}, & n \text{ odd} \end{cases}
$$

(65)

are the locations of the maxima of the n-th order Chebyshev response (i.e., the values of the frequency ω for which the ripple γ of the magnitude squared response of Chebyshev filters $|H_{Cn}(\omega)|^2$ is at its maximum). In addition, we have

$$
\max_{\omega \in [1-a, 1+a)} |H_n(\omega)|^2 = \begin{cases} (K_{1C} + K_{2C})^2 & \text{if } 1-a < \omega_{max}(n,0) \\ |H_n(\omega)|^2 \big|_{\omega = 1-a} & \text{if } 1-a \geq \omega_{max}(n,0) \end{cases}
$$

(66)

and

$$
\max_{\omega \in [1+a, \infty)} |H_n(\omega)|^2 = |H_n(\omega)|^2 \big|_{\omega = 1+a}
$$

(67)

We note that $\omega_{max}(n,0)$ and $\omega_{max}(n,k_{max})$ are, respectively, the largest and smallest values of ω ($0 \leq \omega \leq 1$) for which $|H_{Cn}(\omega)|^2$ reaches its maximum (see Eqs. (48), (49), and Figs. 9(a)-(c)).

Similarly, we have

$$\underset{\omega \in [\,0,\ 1-a)}{\text{Max}} \ \left|1-H_n(\omega)\right|^2 = \left(1 - \frac{K_{1C}}{1 + \beta^2} - K_{2C}\right)^2 \tag{68}$$

$$\underset{\omega \in [\,1-a,\ 1+a)}{\text{Max}} \ \left|1-H_n(\omega)\right|^2 = \left|1-H_n(\omega)\right|^2\bigg|_{\omega \,=\, 1+a} \tag{69}$$

and

$$\underset{\omega \in [\,1+a,\ \infty)}{\text{Max}} \ \left|1-H_n(\omega)\right|^2 = \left|1-H_n(\omega)\right|^2\bigg|_{\omega \,=\, +\infty}$$

$$= \left(1 - K_{2C}\right)^2 \tag{70}$$

We observe that $(K_{1C} + K_{2C})^2$ and $\left(1 - \dfrac{K_{1C}}{1 + \beta^2} - K_{2C}\right)^2$ are the maximum values of the ripples of $\left|H_n(\omega)\right|^2$ and $\left|1-H_n(\omega)\right|^2$, respectively.

Substituting Eqs. (64)-(70) in Eq. (62) for the approximate robust filter $H_n(\omega)$ with the Chebyshev approximation and using the optimal value of a for each order n and each ripple γ, we can obtain the worst-case output SNR's (as given by Eq. (43.b) for the p-point classes $\mathscr{A}_p$ and $\mathcal{N}_p$) for the filters $H_n(\omega)$, n=2,3,...,10, and ripples γ = 0.5, 1, 2, and 3 dB. Figures 11(a), (b), (c), and (d) illustrate the worst-case performances of the approximate robust filters $H_n(\omega)$ for values of the ripple γ = 0.5, 1, 2, and 3 dB respectively, compared to the worst-case performance of the ideal robust filter H_R, and trivial filtering. We observe that, for a fixed value of the ripple γ, performance improves with increased order n. This is to be expected since, for a given ripple γ, as the order n increases, the rolloff of $\left|H_{Cn}(\omega)\right|^2$ in the stopband is steeper (see Figs. 9(a), (b), and (c)), and therefore the approximate robust filter's response is closer to that of the ideal robust
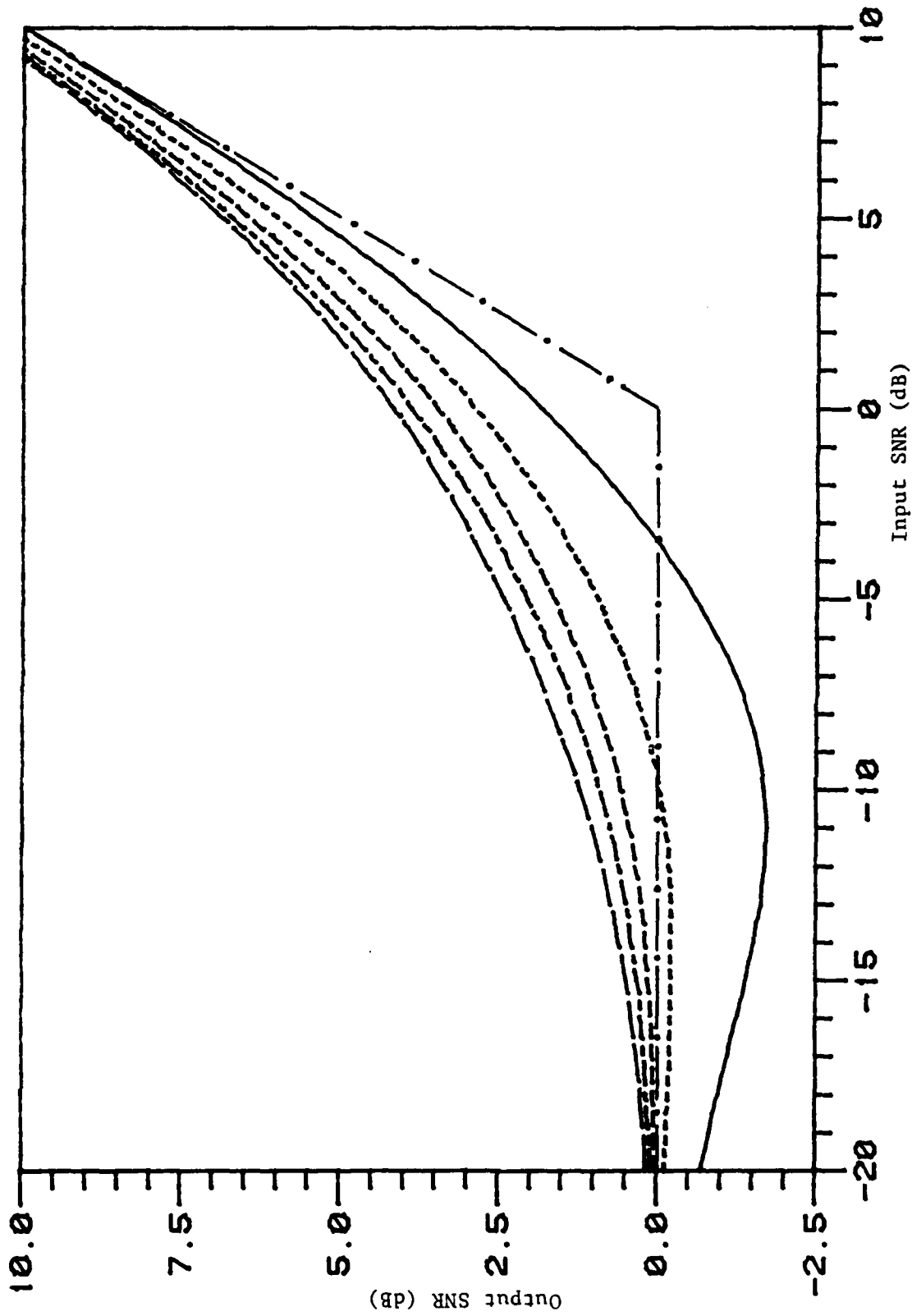
Figure 11(a). p-Point class. Chebyshev approximation (Fixed ripple $\gamma = 0.5$dB). (From top to bottom) Worst-case performances of ideal robust filter H_R, and approximate robust filters H_n, n=10, 5, 3, and 2.
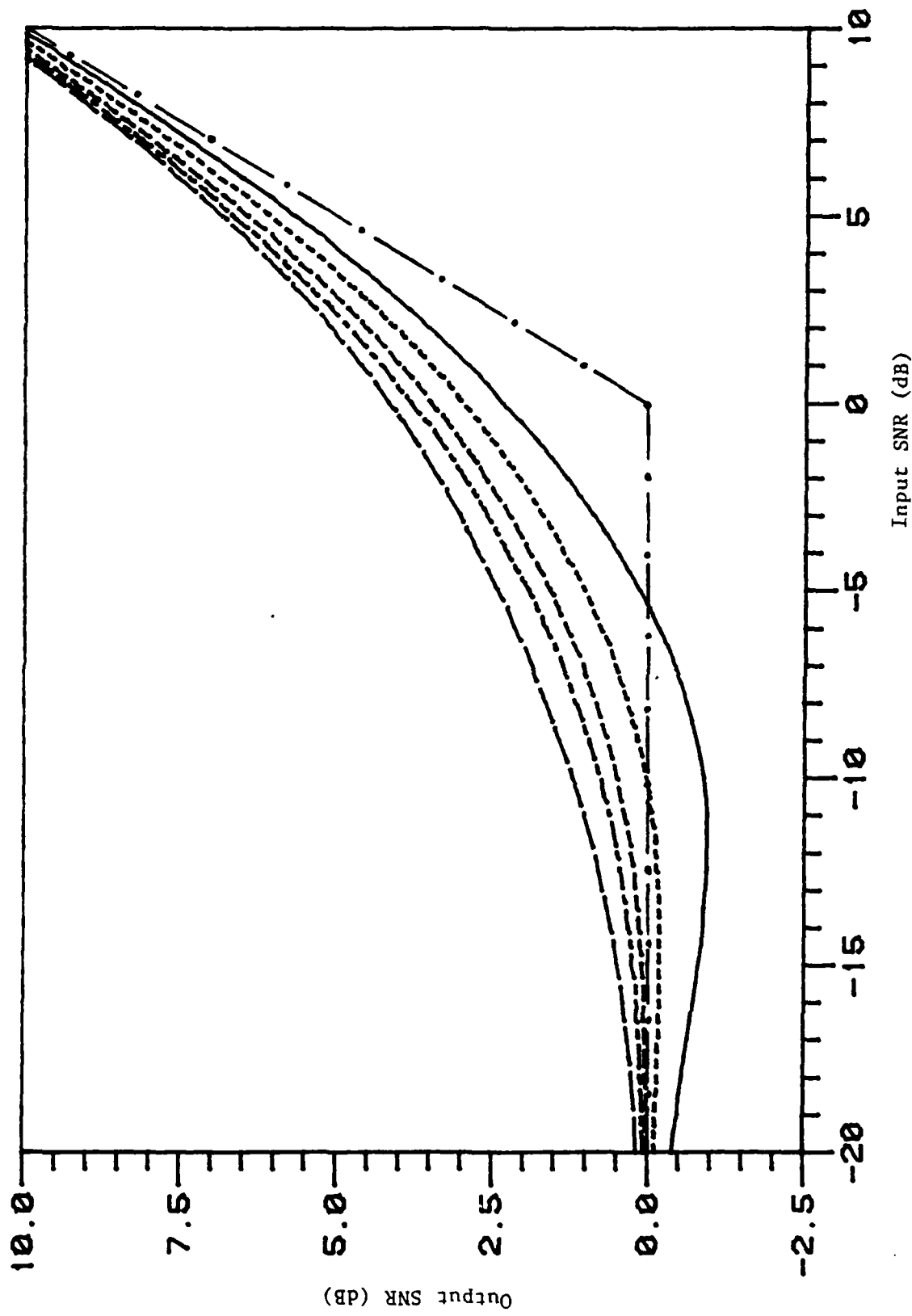
Figure 11(b). p-Point class. Chebyshev approximation ($\gamma = 1$dB). (From top to bottom) Worst-case performance of ideal robust filter H_R, and approximate robust filters H_n, n=10, 5, 3, and 2.
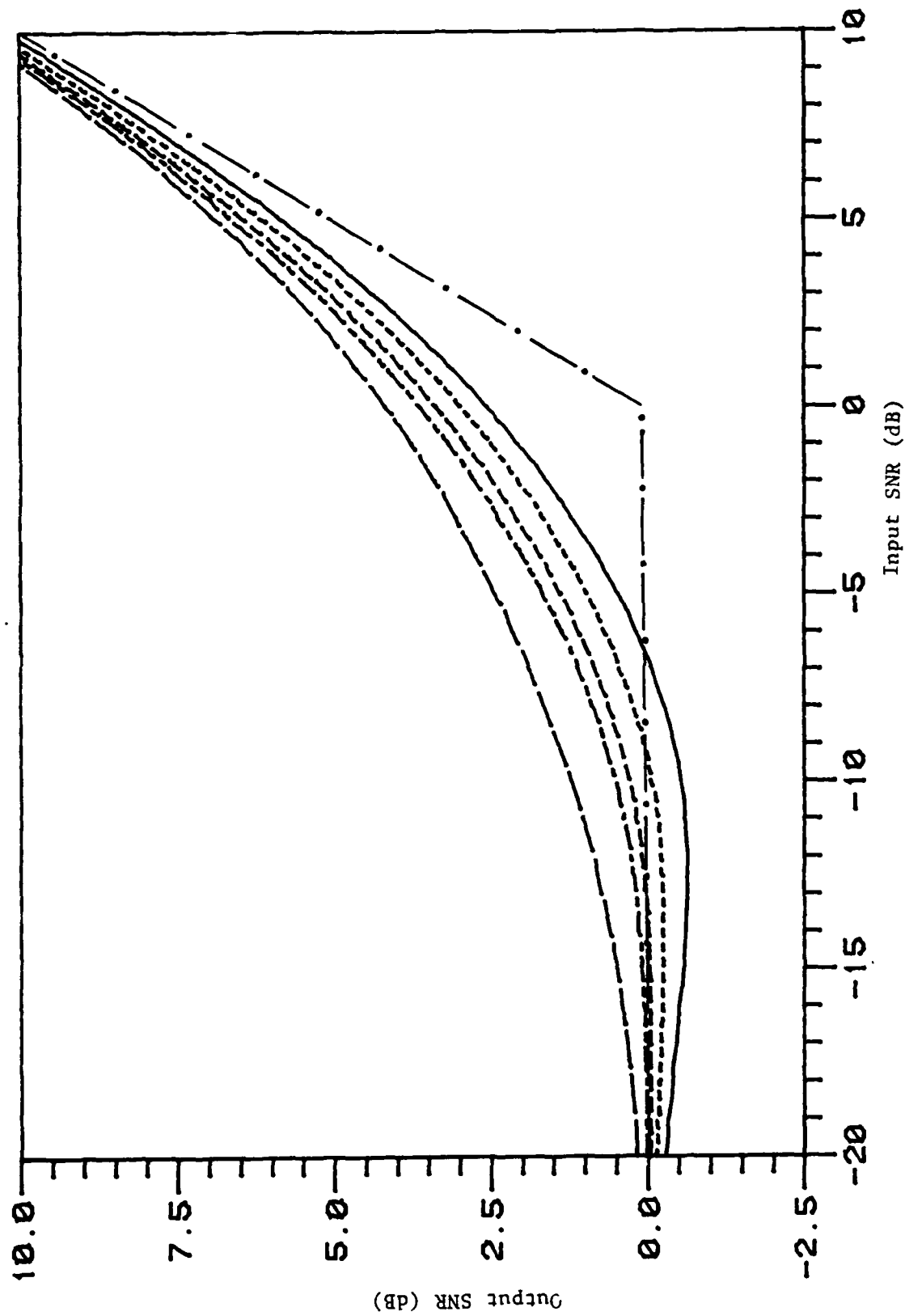
Figure 11(c). p-Point class. Chebyshev approximation (γ =2dB). (From top to bottom) Worst-case performances of ideal robust filter H_R, and approximate robust filters H_n, n=10, 5, 3, and 2.
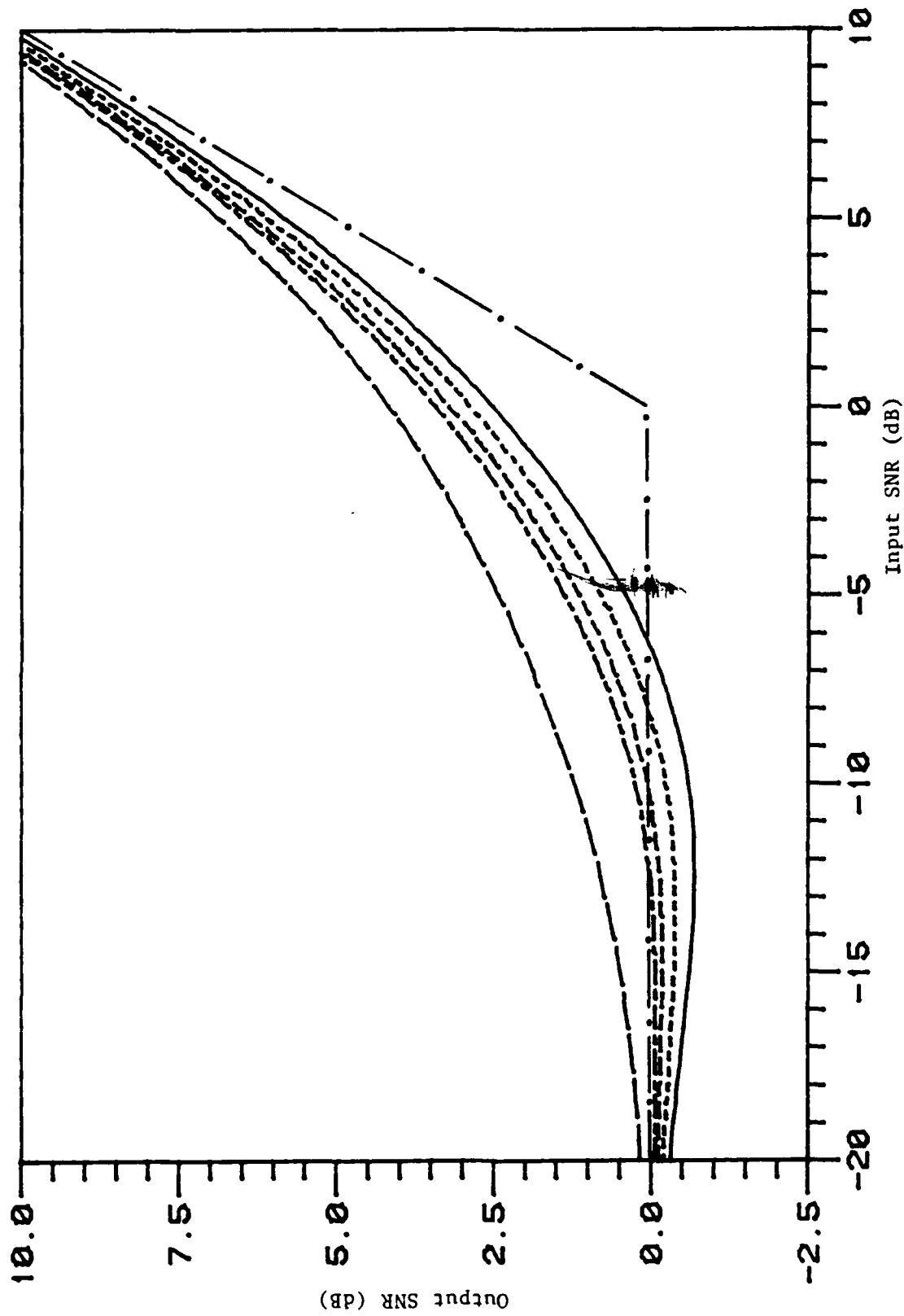
Figure 11(d). p-Point class. Chebyshev approximation (γ =3dB).(From top to bottom) Worst-case performances of ideal robust filter H_R, and approximate robust filters H_n, n=10, 5, 3, and 2.

filter. In comparing Figs. 11(a), (b), (c), and (d), we see that, except for very small orders (n=2 and 3), the filters $H_n(\omega)$ with the smaller ripple (γ = 0.5 dB) have the best performance. For the second and third order filters, there is an improvement in performance with increased ripple. To get more insight on the effect of the ripple on performance, we have compared the worst-case output SNR for $H_n(\omega)$ with different values of the ripple, when the order n is fixed. Figures 12(a), (b), (c), (d), and (e) illustrate the worst-case performances of the approximate robust filter $H_n(\omega)$ for n = 2, 3, 5, 7, and 10, respectively, and several values of the ripple γ (0.1 dB $\leq$ $\gamma \leq$ 3 dB).

In Figure 12(a) (n=2), we see that, for such a small order n, the improvement in performance due to a steeper rolloff in the stopband, as the ripple γ is increased, is greater than the deterioration in performance due to a larger value of the peak of the ripple in the passband (see Figs. 9(a), (b), and (c)). Thus, the general effect, in this case, is that increasing the ripple improves worst-case performance. The only exception to this is that performance for γ = 3 dB (which is not shown) is slightly worse than for γ = 2 dB, because the difference in rolloff between the two ripples is smaller than the difference in the maximum of the ripple. Results for γ = 0.1 dB are not shown but are much worse than for γ = 0.5 dB, due to the compounded effect of a small ripple and a small order n, both leading to a very gradual rolloff.

In Figure 12(b) (n=3), the tradeoff between increasing the ripple to get a more abrupt rolloff in the stopband and decreasing the ripple to lower the maximum value of its peak in the passband, is more apparent.
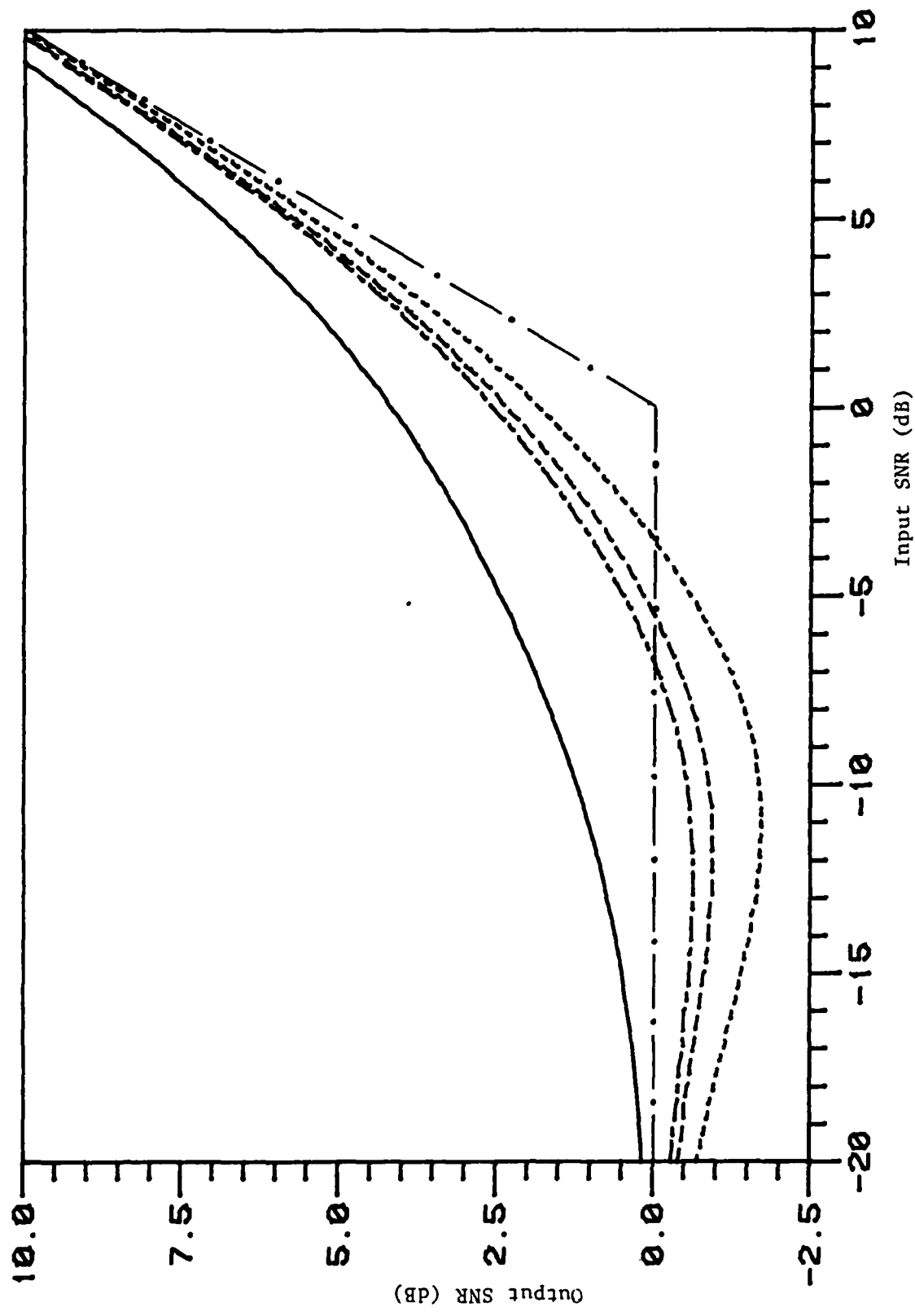
Figure 12(a).   p-Point class.   Chebyshev approximation (Fixed order n = 2). (From top to bottom) Worst-case performances of ideal robust filter H_R and approximate robust filters H_2 for ripples $\gamma = 2$, 1, and 0.5 dB.
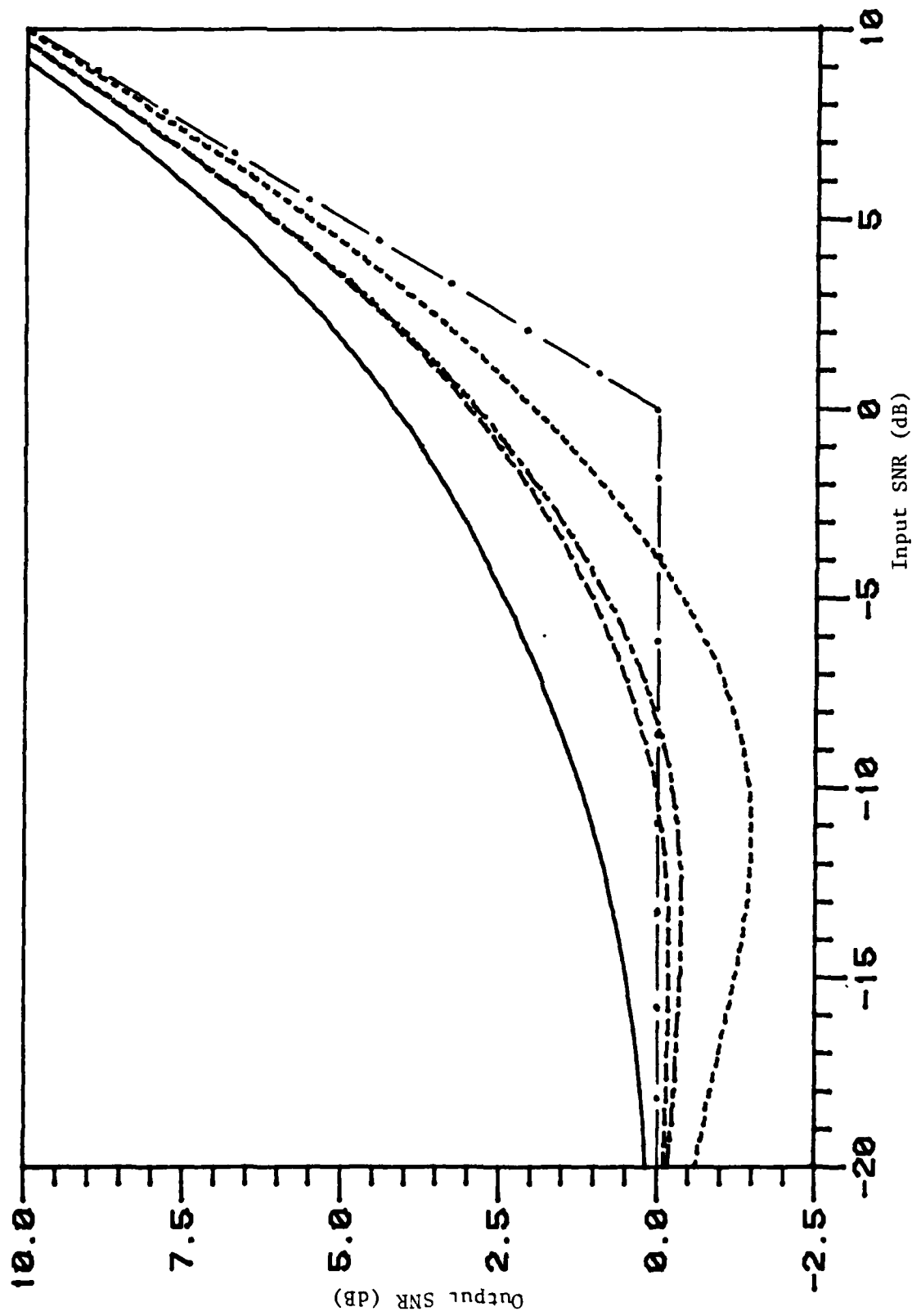
Figure 12(b). p-Point class. Chebyshev approximation (n=3). (From top to bottom) Worst-case performances of ideal robust filter H_R and approximate robust filters H_3 for $\gamma=1$, 3, and 0.1 dB.

Figure 12(c). p-Point class. Chebyshev approximation (n=5). (From top to bottom) Worst-case performances of ideal robust filter H_R and approximate robust filters H_5 for $\gamma=0.5$, 2, and 3 dB.
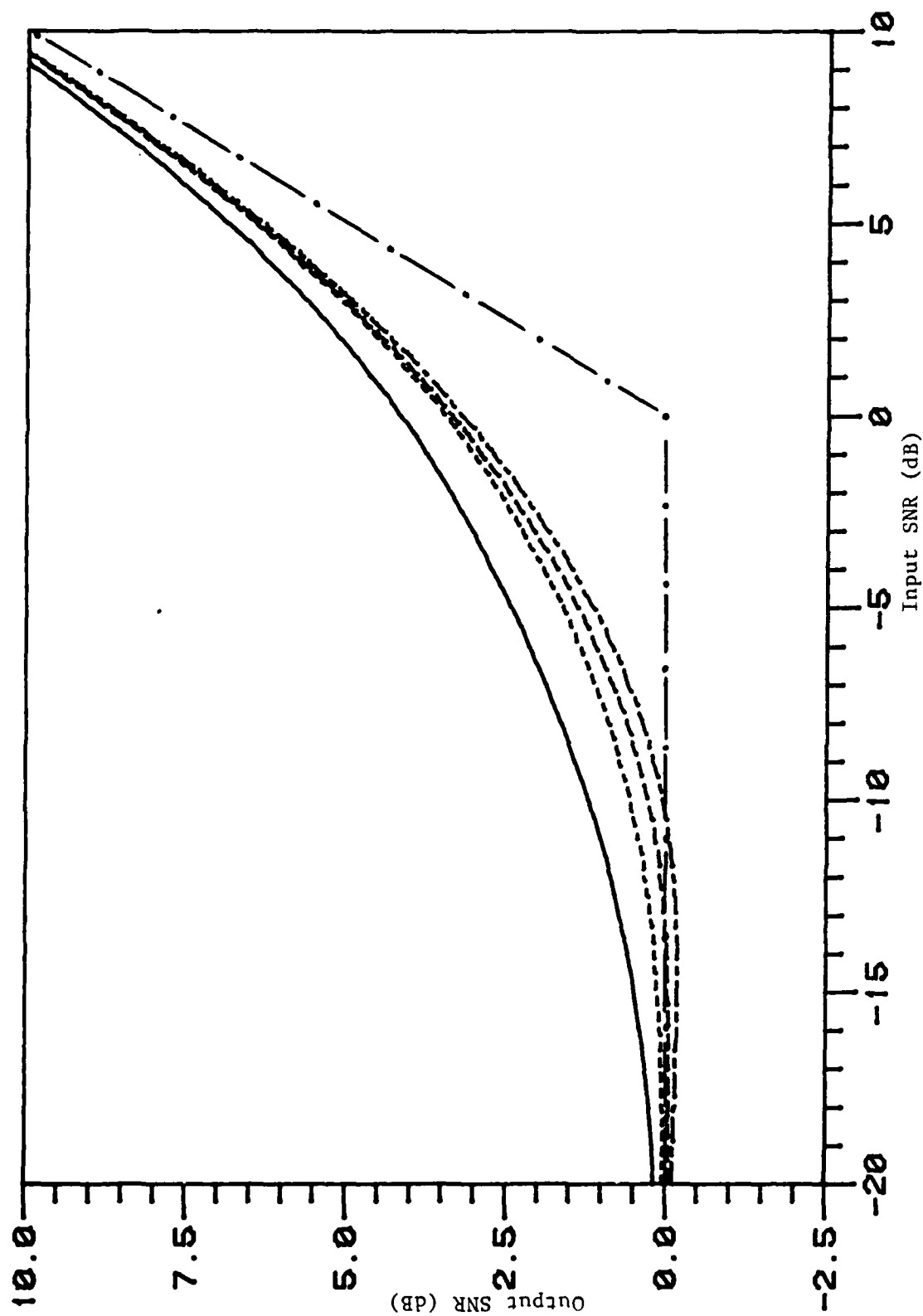
Figure 12(d). p-Point class. Chebyshev approximation (n=7). (From top to bottom) Worst-case performances of ideal robust filter H_R and approximate robust filters H_7 for $\gamma=0.5$, 1, 2, and 3 dB.
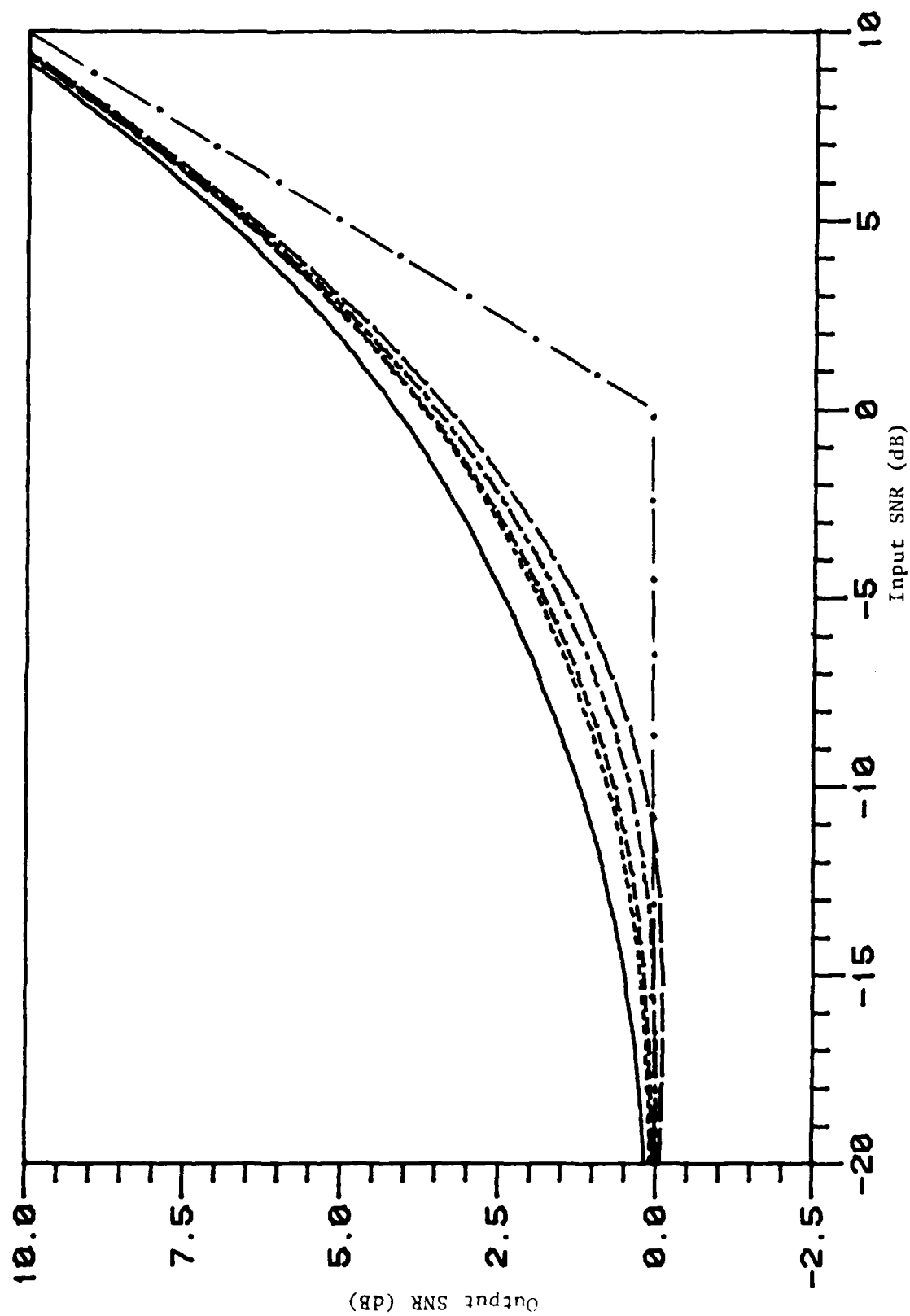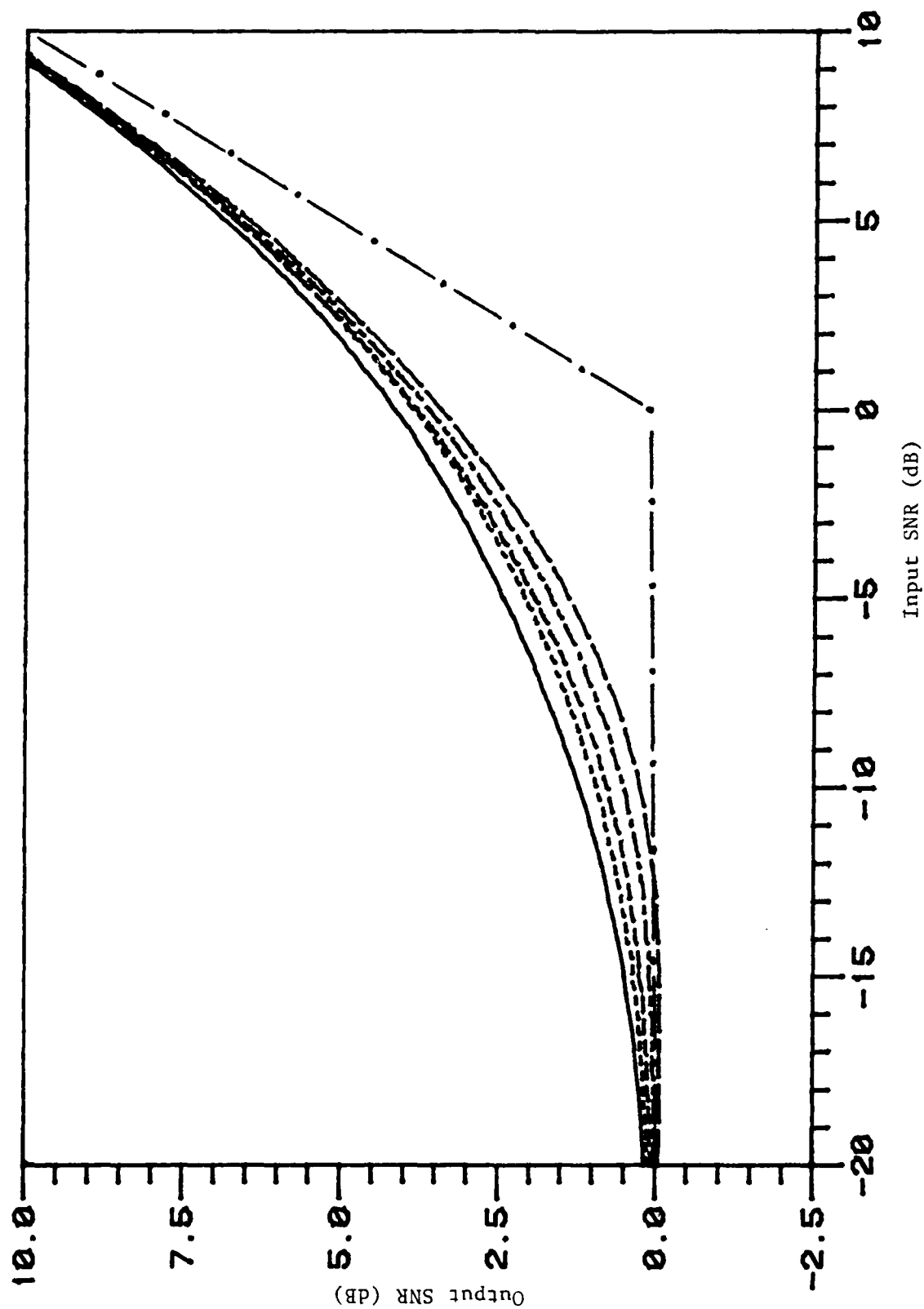
Figure 12(e). p-Point class. Chebyshev approximation (n=10). (From top to bottom) Worst-case performances of ideal robust filter H_R and approximate robust filter H_{10} for $\gamma=0.1$, 1, 2, and 3 dB.

Performance for γ=2 and 0.5 dB (both not shown) is almost the same and falls between the γ=1 and 3 dB curves.

In Figure 12(c) (n=5), we observe that, in general, the results are substantially better than for n=2 and 3. Furthermore, since the rolloff in the stopband is already much steeper because of the higher order, a larger ripple for the filters $H_n(\omega)$ contributes more to a degradation in perform- ance due to the large peak in the passband than to an improvement due to the steeper rolloff in the stopband. The reason for this is that, as seen in Figs. 9(a), (b), and (c), as the order n increases, the improvement in rolloff due to a larger ripple decreases. We note that the best performance is obtained for γ = 0.5 dB, followed very closely by γ = 1 dB (not shown). Performance for the smallest ripple considered, γ = 0.1 dB, is not shown, but our results indicate that it is between the γ=1 and 2 dB curves towards the negative input SNR's (in dB), then almost coincides with the 3 dB curve towards positive SNR's (in dB). This effect indicates that the improvement in rolloff due to an increased ripple is more pronounced for positive input SNR's. Indeed, this is the case, since, if we look at the term

$$P_{Nj} \max_{\omega \in I_j} |H_n(\omega)|^2 / r \tag{71}$$

in Eq. (62), we observe that the interval I_j over which this term has the greatest contribution is $I_3 = [1+a, \infty)$ because the noise has a 3 dB band- width at ω=10, and thus the largest fraction of its power is p_{N3} (in the interval I_3). From Equation (67), it is clear that this maximum reflects the effect of the rolloff of $|H_n(\omega)|^2$ in the stopband. For positive input SNR's (in dB), i.e., r>1, since the maximum is divided by r, the term in

(71) is further decreased, leading to better performance.

Finally for $n \geq 7$ (see Figs. 12(d) and (e) for n=7 and 10, respectively), performance improves with decreasing ripple with the best performance obtained for ripples γ = 0.5 or 0.1 dB. For high orders n, the predominant effect is the peak value of the ripple in the passband, because the rolloff is already abrupt and the improvement in rolloff due to an increased ripple is relatively small.

By plotting figures similar to Figures 12(a)-(e) for all n (n=2,3,...,10), it is possible to find for each n, the value of the ripple that gives the best performance for this filter and the one that gives the worst performance. These values are shown in Table 1. From these results, we conclude that ripples γ larger than 2 dB or smaller than 0.1 dB should not be considered, since the 3 dB ripple yields the worst performances for all n except 2 and 3, and the 0.1 dB ripple has good performances only for orders $n \geq 7$ and the worst performances for n=2 and 3. In addition, we observe that the larger values of the ripple (γ = 2 and 1 dB) yield the best performance for small orders n, while small values of the ripple (γ = 0.1 and 0.5 dB) yield the best performance for large orders n. Again, this reflects the fact that for small n the improvement gained from a steeper folloff in the stopband due to a larger ripple is greater than the deterioration from a larger maximum of the ripple in the passband. For large n, the opposite is true.

5. Comparison of the Butterworth and Chebyshev approximations

   and conclusions

In order to compare the performances of the approximate robust filters using the Butterworth or Chebyshev approximations, we have shown, in Fig. 13, the worst-case performance of the approximate robust filter H_n with the

TABLE 1

VALUES OF THE RIPPLE γ (IN dB) THAT GIVE THE BEST AND
WORST PERFORMANCE FOR EACH APPROXIMATE ROBUST FILTER
$H_n(\omega)$ (USING THE CHEBYSHEV APPROXIMATION) FOR THE
p-POINT CLASS

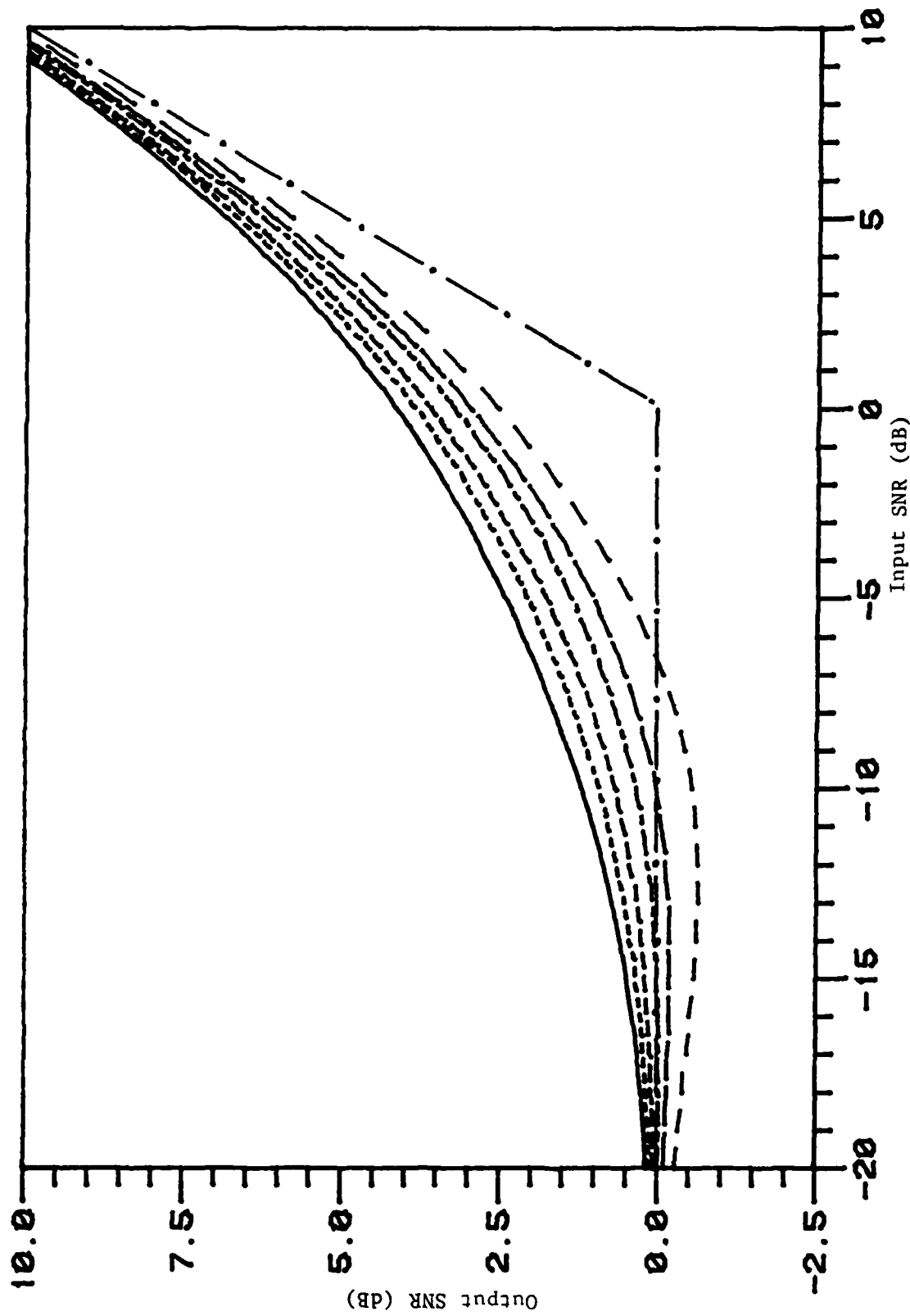| n	Best ripple (dB)	Worst ripple (dB)
2	2	0.1
3	1	0.1
4	0.5, 1	3 (input snr < -3dB) 0.1 (input snr > -3 dB)
5	0.5 (1 slightly worse)	3
6	0.5	3
7	0.5 (0.1 slightly worse)	3
8	0.5 (0.1 slightly worse)	3
9	0.5, 0.1	3
10	0.1 (0.5 slightly worse)	3

Figure 13. p-Point class. Chebyshev approximation. (From top to bottom) Worst-case performances of ideal robust filter H_R and approximate robust filters H_n, n=10,6,4,3, and 2 with the optimal values of the ripple γ for each n (as given in Table 1).

Chebyshev approximation and the value of the ripple γ that gives the best performance for each order n (see Table 1). From Figs. 10 and 13, it is clear that, except for n=4 where both approximations yield about the same results, the Chebyshev approximation gives better performance than the Butterworth approximation for $n \geq 5$ and vice versa for n=2 and 3. The justification for these results is that, for $n \geq 5$, the Chebyshev response has substantially larger attenuations near the cutoff frequency $\omega_c = 1$ in the stopband than the Butterworth response (see Figs. 2, 9(a)-(c)). However, for n=2 and 3, although the Chebyshev response is in general steeper than the Butterworth response, the attenuation near $\omega_c = 1$ in the stopband is greater for the Butterworth response $|H_{Bn}(\omega)|^2$ because at $\omega_c = 1$ the Butterworth response has dropped to a lower value than the Chebyshev response.

The general conclusion that can be drawn for the p-point class is that for orders $n \geq 5$, the approximate robust filters using the Chebyshev approximation and the corresponding optimal value of γ for each n, have a worst-case performance that is sufficiently close to that of the ideal robust filter H_R, particularly for the higher orders n (less than 0.7 dB difference for n=7 and less than 0.4 dB difference for n=10). For orders n = 2, 3, and 4, the Butterworth approximation yields better results (or equal for n=4) than the Chebyshev approximation. These filters with small orders n have a worst-case performance that is better than trivial filtering except for a small portion of the negative input SNR axis. Thus, in the worst-case they have even better performance than the nominal filter H_0^*.

IV. SUMMARY AND CONCLUSIONS

In this study, we have approximated the ideal robust Wiener filters for both the ε-contaminated and the p-point uncertainty classes of spectra with realizable n-th order filters of the Butterworth and Chebyshev types. The worst-case performance of the approximate robust filters was compared to that of the corresponding ideal robust filter.

In the ε-contaminated class the uncertainty is modeled in terms of contaminating densities which modify to a certain degree the nominal densities of the signal and noise. For this class we have shown that the approximate robust filter using only second order Butterworth low-pass filters gives a very good approximation to the ideal robust filter for that class, for both degrees of uncertainty considered (less than 0.2 dB difference).

In the p-point class the only knowledge of the PSD's of the true signal and noise is their total and fractional powers. Here we have considered two approximations, using either Butterworth or Chebyshev filters. The Butterworth approximate robust filters have a worst-case performance which gradually approaches that of the ideal robust filter with increasing order n (within 0.7 dB for n = 10). The Chebyshev approximate robust filters also have a worst-case performance which improves with increasing order n, for a given ripple γ. In addition, we observed that there is a tradeoff between increasing the ripple of the Chebyshev filters to improve the rolloff in the stopband and decreasing the ripple to decrease its maximum value in the passband. For different orders n, one or the other of these two effects is predominant. The result is that the best approximation is obtained for high orders n ($n \geq 7$)

and small ripple (γ = 0.5 or 0.1 dB). We have also shown that the Chebyshev approximate robust filters have better performance than the Butterworth approximate robust filters for higher orders n (n $\geq$ 5) and vice versa for orders n = 2, 3, and 4. Therefore, for the p-point class we conclude that the approximate robust filters using Chebyshev filters of high order and small ripple yield the best approximation to the ideal robust filter (within 0.4 dB for n = 10 and γ = 0.1 dB).

Finally, in comparing the two uncertainty classes of spectra considered, we note that better results have been obtained for the ε-contaminated class than for the p-point class. The reason for this is that there is more uncertainty in the knowledge of the true spectra of the signal and noise in the p-point class than in the ε-contaminated class. .

APPENDIX A

IMPLEMENTATION OF THE MAGNITUDE SQUARED RESPONSE $|H(j\omega)|^2$ OF A CAUSAL FILTER $H(j\omega)$ BY SIGNAL PROCESSING TECHNIQUES

Given a causal filter $H(j\omega)$ with impulse response $h(t)$, we know, from the algebra of complex numbers, that its magnitude squared response can be written as

$$|H(j\omega)|^2 = H(j\omega) \cdot H^*(j\omega) \tag{72}$$

where $H^*(j\omega)$ denotes the complex conjugate of $H(j\omega)$. On the other hand, we know from the properties of Fourier transforms that

$$\mathcal{F}^{-1}[H^*(j\omega)] = h(-t) \tag{73}$$

where $\mathcal{F}^{-1}[H(j\omega)]$ denotes the inverse Fourier transform of $H(j\omega)$. Thus, using the time convolution property of Fourier transforms, we have

$$\mathcal{F}^{-1}[H(j\omega) \cdot H^*(j\omega)] = h(t) * \hat{h}(t) \triangleq \int_{-\infty}^{\infty} h(t-\tau)\hat{h}(\tau)d\tau \tag{74}$$

where

$$\hat{h}(t) \triangleq h(-t) \tag{75}$$

The problem of implementing $|H(j\omega)|^2$ is then equivalent to the time domain convolution of $h(t)$ with $\hat{h}(t)$, as shown in Fig. 14. Thus, if $z(t)$ is the desired output and $y(t)$ is the input, we have

$$z(t) = h(t) * \hat{h}(t) * y(t)$$
$$= (h * y)(t) * \hat{h}(t) \tag{76}$$

Defining

$$x(\sigma) \triangleq (h * y)(\sigma)$$
$$= \int_{-\infty}^{\infty} h(\sigma-\tau)y(\tau)d\tau \tag{77}$$

$y(t) \longrightarrow \boxed{h(t)} \longrightarrow \boxed{\widehat{h}(t)} \longrightarrow z(t)$
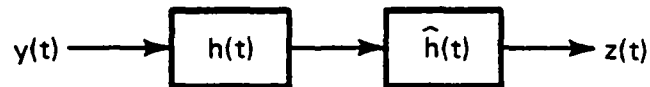
Figure 14. Time domain equivalent of the implementation of $|H(j\omega)|^2$.

$y(t) \longrightarrow \boxed{h(t)} \xrightarrow{x(t)} \boxed{\text{"Reverse Tape"}} \xrightarrow{x(-t)} \boxed{h(t)} \xrightarrow{z(-t)} \boxed{\text{"Reverse Tape"}} \longrightarrow z(t)$

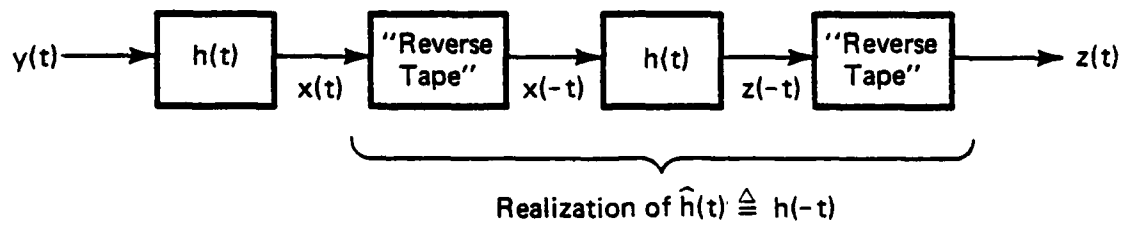Realization of $\widehat{h}(t) \triangleq h(-t)$

Figure 15. Implementation of $|H(j\omega)|^2$ in the time domain by signal processing techniques.

(since $h(\sigma-\tau) = 0$ for $\tau > \sigma$ from the causality of $h(t)$), Eq. (76) becomes

$$z(t) = \int_{-\infty}^{\infty} \hat{h}(t-\sigma)x(\sigma)d\sigma$$

$$= \int_{t}^{\infty} \hat{h}(t-\sigma)x(\sigma)d\sigma \qquad (78)$$

(since $\hat{h}(t-\sigma) = 0$ for $\sigma < t$). Using Eq. (75), we obtain

$$z(t) = \int_{t}^{\infty} h(\sigma-t)x(\sigma)d\sigma. \qquad (79)$$

With the change of variables $\sigma' = -\sigma$, the integral in (79) becomes

$$z(t) = \int_{-\infty}^{-t} h(-\sigma'-t)x(-\sigma')d\sigma' \qquad (80)$$

Therefore,

$$z(-t) = \int_{-\infty}^{t} h(t-\sigma')x(-\sigma')d\sigma' \qquad (81)$$

From the definition of the convolution integral and the causality of $h(t)$, the right-hand side of Eq. (81) is simply the convolution of $h(t)$ with $x(-t)$, i.e.,

$$z(-t) = h(t) * x(-t) \qquad (82)$$

Using Eqs. (77) and (82), we can obtain an implementation of the convolution in Eq. (76) by signal processing techniques, as shown in Fig. 15, where we assume that the data such as $x(t)$ or $z(-t)$ are stored on tape so that $x(-t)$ and $z(t)$ can be obtained by simply reversing the corresponding tape. In this way, we have shown that it is possible to implement $|H(j\omega)|^2$ (although not in real time).

APPENDIX B

ROLE OF THE PARAMETER a IN THE PARTICULAR p-POINT
CLASS CONSIDERED AND OPTIMAL CHOICE OF a

The purpose of this appendix is to justify the introduction of a small
interval $[1-a, 1+a]$ around the breakpoint $b_1 = 1$ in the p-point class used by
Vastola [3] as described in Chapter III, Section B.1 (with $m = 2$, $b_0 = 0$,
$b_1 = 1$, and $b_2 = +\infty$), and to show how the parameter a was chosen optimally for
each approximate robust filter considered.

The modified p-point class has three regions ($m = 3$) with the breakpoints
$b_0 = 0$, $b_1 = 1-a$, $b_2 = 1+a$, and $b_3 = +\infty$. The expression for the worst-case
MSE for this class is given by Eq. (58). For the p-point class considered by
Vastola [3], the expression is the same except that the limit of the summation
is 2 instead of 3. From Eqs. (52) and (53), and Figs. 2, 9(a) - 9(c), we
observe that the responses of the approximate robust filters (with the
Butterworth approximation or the Chebyshev approximation for a given ripple γ)
have the same value at $\omega = 1$ for all orders n. Thus, it is clear that the
maxima in Eq. (58) (for the p-point class considered by Vastola [3]) will be
the same for all orders n of the Butterworth approximate robust filters or of
the Chebyshev approximate robust filters with a given ripple γ. Therefore,
by using the $m = 2$ p-point class with the breakpoint $b_1 = 1$, we are not able
to distinguish the improvement in worst-case performance when the order of the
approximate robust filters is increased. This observation led us to introduce
a small interval $[1-a, 1+a]$ around $\omega = 1$ and choose the parameter a in an
optimal way.

Since the desired intermediate region is to be small, we confined a to

lie in the interval [0,0.4]. The procedure for choosing the optimal value of

the parameter a is the following: for a fixed input SNR and for each

approximate robust filter, the output SNR is computed for all values of a,

$0 \leq a \leq 0.4$. The value of a which yields the maximum output SNR is chosen to

be the optimal value of a for the particular approximate robust filter

considered.

By fixing the input SNR at several values and repeating the above procedure,

we found that the optimal values of a are relatively insensitive to changes in

input SNR. Thus, in our numerical results, we fixed the input SNR at 0 dB.

For the approximate robust filters using the Butterworth approximation, we

repeat the above procedure for each order n. Figure 16 shows the variations

of the worst-case output SNR with the parameter a, for the ideal robust filter

H_R, and the approximate robust filters H_n using the Butterworth approximation

for several orders n (with the input SNR fixed at 0 dB). We observe that, for

small orders n, a larger value of a yields better performance because the

rolloff of the filters with small n is very gradual. As n increases, a smaller

value of a is optimal. We also note that the ideal robust filter's worst-

case output SNR is relatively insensitive to variations in the parameter a.

Therefore, in our numerical results, we have used a value of a = 0 for the

ideal robust filter. Table 2 shows the optimal values of a for each approximate

robust filter H_n using the Butterworth approximation.

For the approximate robust filters using the Chebyshev approximation,

we have to choose the optimal value of a (as described above) for each order

n and each ripple γ. Figures 17(a), (b), and (c) show the variations of the

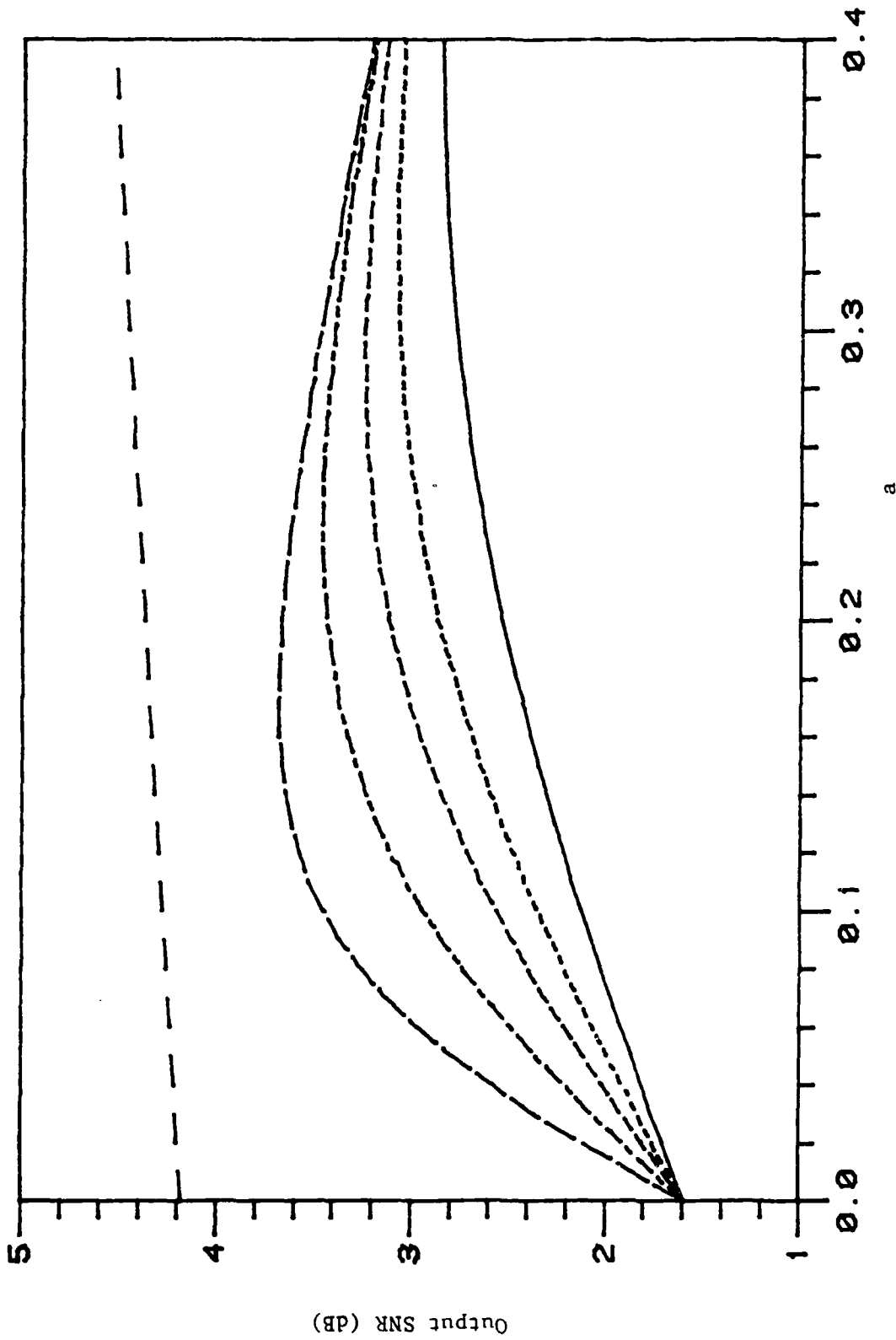worst-case output SNR with the parameter a, for the approximate robust filters

Figure 16. p-Point class. Butterworth approximation. (From top to bottom) Worst-case output SNR versus a (fixed input SNR = 0 dB) for the ideal robust filter H_R and the approximate robust filters H_n, n = 10, 6, 4, 3, and 2.

TABLE 2

OPTIMAL VALUES OF THE PARAMETER a FOR THE APPROXIMATE ROBUST
FILTERS H_n WITH THE BUTTERWORTH APPROXIMATION (FOR EACH ORDER n)

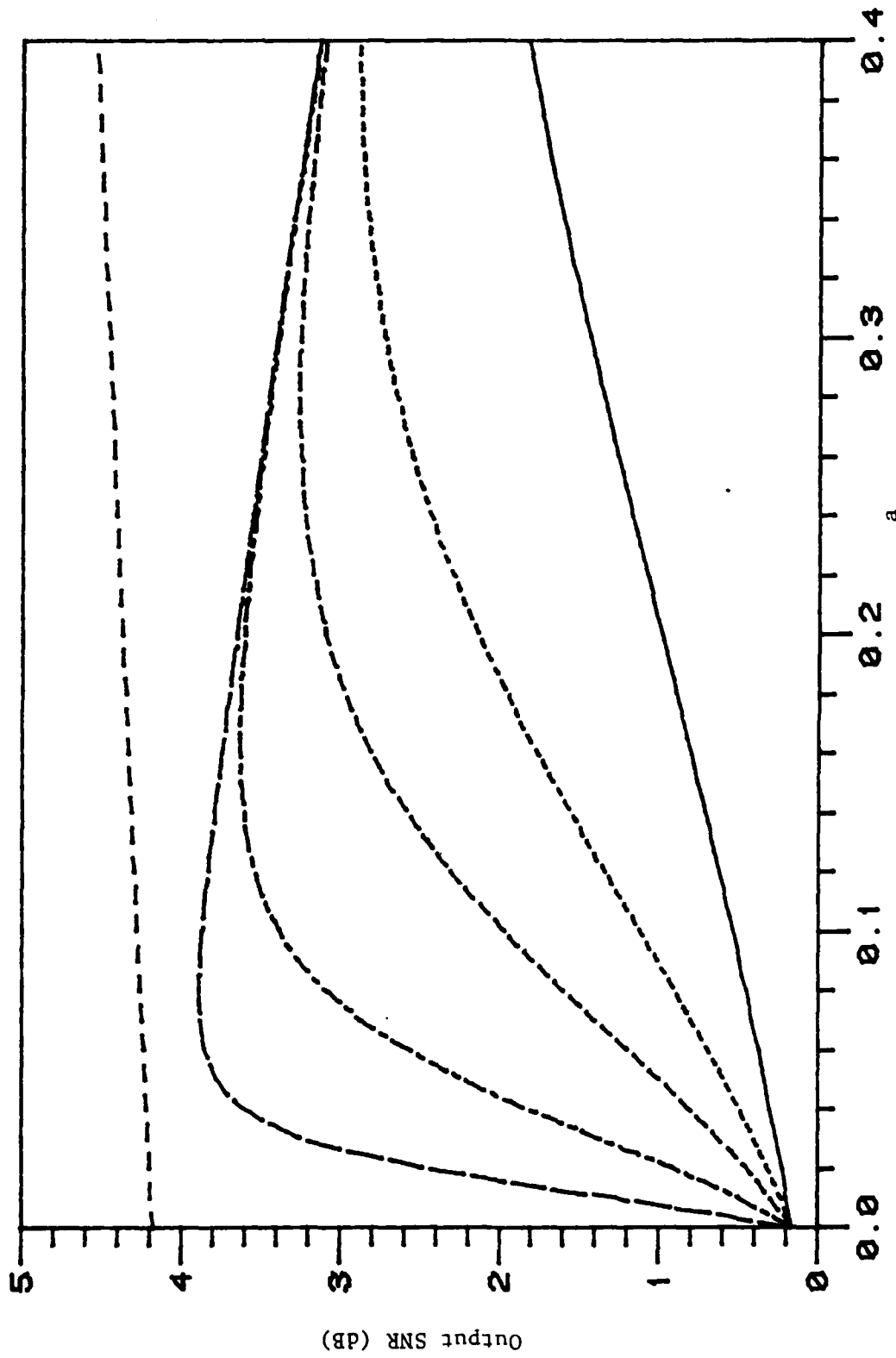| n	Optimal a
2	0.40
3	0.33
4	0.29
5	0.26
6	0.24
7	0.22
8	0.20
9	0.19
10	0.17

Figure 17(a). p-Point class. Chebyshev approximation (γ = 0.5 dB). (From top to bottom) Worst-case output SNR versus a (fixed input SNR = 0 dB) for the ideal robust filter H_R and the approximate robust filters H_n, n = 10, 6, 4, 3, and 2.

Figure 17(b). p-Point class. Chebyshev approximation ($\gamma = 1$ dB). (From top to bottom) Worst-case output SNR versus a (fixed input SNR = 0 dB) for the ideal robust filter H_R and the approximate robust filters H_n, n = 10, 6, 4, 3, and 2.
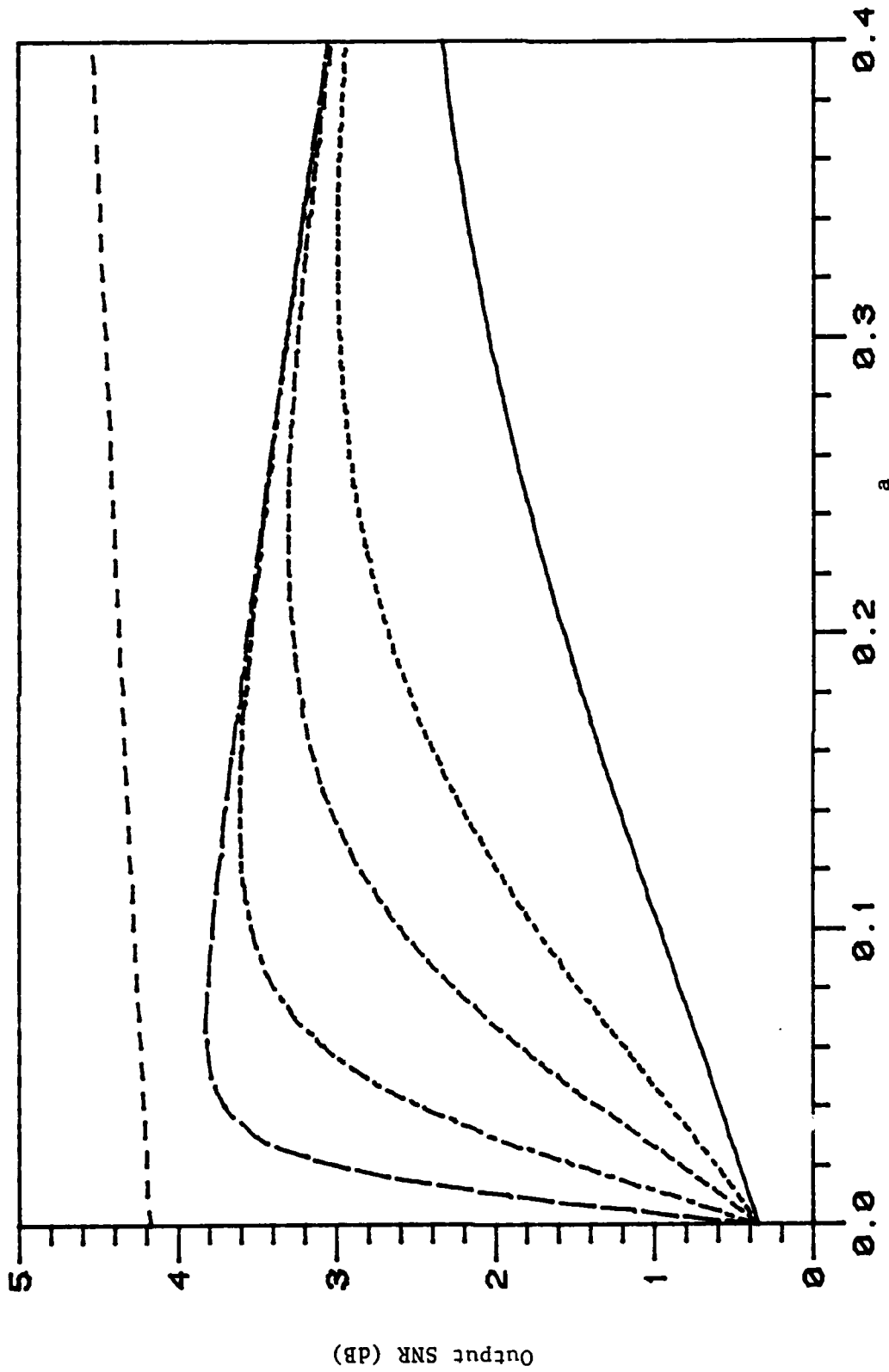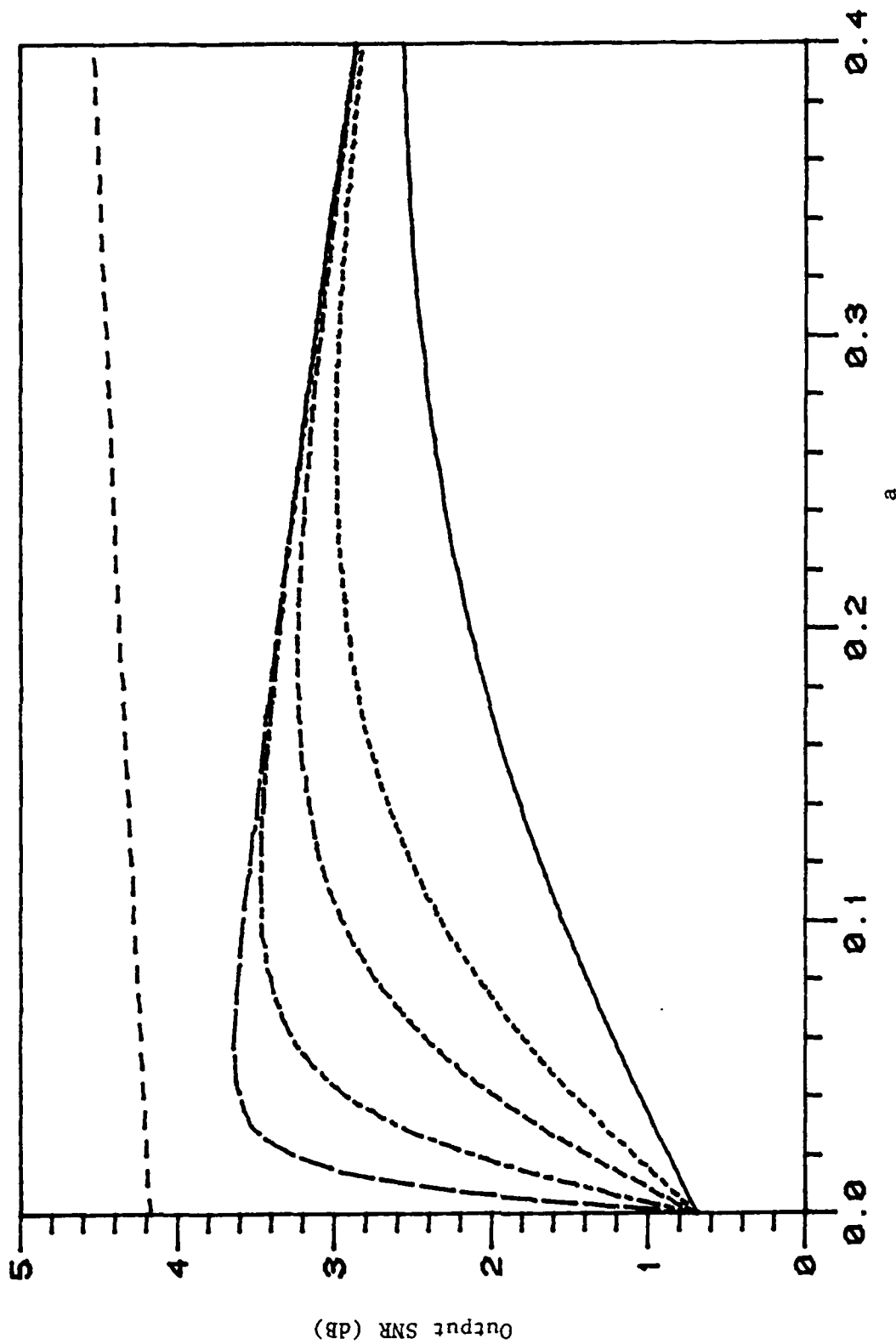
Figure 17(c). p-Point class. Chebyshev approximation (γ = 2 dB). (From top to bottom) Worst-case output SNR versus a (fixed input SNR = 0 dB) for the ideal robust filter H_R and the approximate robust filters H_n, n = 10, 6, 4, 3, and 2.

H_n with the Chebyshev approximation, and for ripples $\gamma = 0.5$, 1 and 2 dB, respectively. In general, the optimal value of a is smaller for larger n and larger ripple γ. Table 3 shows the optimal values of a for the approximate robust filters with the Chebyshev approximation, for each order n and each ripple γ. The optimal values of a in Tables 2 and 3 are the values used in the numerical results of Chapter III.

TABLE 3

OPTIMAL VALUES OF THE PARAMETER a FOR THE APPROXIMATE ROBUST
FILTERS H_n WITH THE CHEBYSHEV APPROXIMATION
(FOR EACH ORDER n AND EACH RIPPLE γ)

γ(dB)	0.1	0.5	1	2	3
n			Optimal a		
2	0.400	0.400	0.400	0.400	0.370
3	0.400	0.400	0.330	0.265	0.225
4	0.400	0.280	0.235	0.190	0.165
5	0.300	0.210	0.175	0.145	0.125
6	0.235	0.165	0.140	0.115	0.100
7	0.185	0.135	0.115	0.095	0.080
8	0.155	0.110	0.095	0.080	0.070
9	0.130	0.095	0.080	0.065	0.060
10	0.110	0.080	0.070	0.055	0.050

REFERENCES

1. H. V. Poor, "On robust Wiener filtering," *IEEE Trans. Automat. Contr.*, Vol. AC-25, pp. 531-536, 1980.

2. S. A. Kassam and T. L. Lim, "Robust Wiener filters," *J. Franklin Inst.*, Vol. 304, pp. 171-185, 1977.

3. K. S. Vastola and H. V. Poor, "An analysis of the effects of spectral uncertainty on Wiener filtering," *Automatica*, Vol. 19, No. 3, pp. 289-293, 1983.

4. P. J. Huber, "A robust version of the probability ratio test," *Ann. Math. Statist.*, Vol. 36, pp. 1753-1758, 1965.

5. Y. Hosoya, "Robust linear extrapolations of second-order stationary processes," *Ann. Prob.*, Vol. 6, pp. 574-584, 1978.

6. J. W. Tukey, "A survey of sampling from contaminated distributions," in *Contributions to Probability and Statistics* (I. Olkin, editor), pp. 448-485, Stanford: Stanford Univ. Press, 1960.

7. S. A. Kassam, "Robust hypothesis testing for bounded classes of probability densities," *IEEE Trans. Inform. Theory*, Vol. IT-27, pp. 242-247, 1981.

8. H. Rieder, "Least-favorable pairs for special capacities," *Ann. Statist.*, Vol. 5, pp. 909-921, 1977.

9. M. E. Van Valkenburg, *Analog Filter Design*. New York: Holt, Rinehart and Winston, 1982.

10. L. J. Cimini and S. A. Kassam, "Robust and quantized Wiener filters for p-point spectral classes," *Proc. 14th Conf. on Inform. Sciences and Systems*, Princeton University, Princeton, NJ, pp. 314-319, 1980.

11. J. W. Craig, *Design of Lossy Filters*. Cambridge, MA: The M.I.T. Press, 1970.

END

FILMED

1-86

DTIC